NASA-CR-190859

SBIR- 08.03-8629A
release date 3/02/92

FINAL REPORT

A SMALL, SINGLE STAGE ORIFICE PULSE TUBE CRYOCOOLER DEMONSTRATION

CONTRACT NO. NAS7-1031

CONTRACT PERIOD: MARCH 2, 1988 THROUGH AUGUST 2, 1990

PREPARED FOR:

NATIONAL AERONAUTICS AND SPACE ADMINISTRATION
JET PROPULSION LABORATORY
PASADENA, CA

PREPARED BY:

DR. JOHN B. HENDRICKS, PRINCIPAL INVESTIGATOR
DR. MYRON E. CALKINS, PROJECT SCIENTIST
ALABAMA CRYOGENIC ENGINEERING, INC.
P.O. BOX 2470
HUNTSVILLE, AL 35804

AUGUST 30, 1990

A SMALL, SINGLE STAGE ORIFICE PULSE TUBE CRYOCOOLER DEMONSTRATION
CONTRACT NO. NAS7-1031

Project Summary

The principal objective of this effort was: "The demonstration of a 0.25 Watt, 80 Kelvin Orifice Pulse Tube Refrigerator." Such a refrigerator has numerous potential scientific, military, and commercial applications.

This program has produced the following results:

a. A partially optimized pulse tube refrigerator has been developed that demonstrates an ultimate temperature of 77K, has a projected cooling power of 0.18 Watts at 80K, and a measured cooling power of 1 Watt at 97K, with an electrical efficiency of 250 Watts / Watt, much better than previous pulse tube refrigerators.

b. A model of the pulse tube refrigerator has been developed that provides estimates of pressure ratio and mass flow within the pulse tube refrigerator, based on component physical characteristics.

c. A model of pulse tube operation has been developed based on generalized analysis. This model is adequate to support local optimization of existing designs.

d. A model of regenerator performance has been developed based on an analogy to counterflow heat exchangers.

The analytical and experimental work in this program supports the following conclusions.

a. Practical pulse tube refrigerators with cooling powers in the range of 0 to 2 Watts are possible, and may be expected to exhibit specific inputs in the 100-250 Watts/Watt range at 90-100K and possibly as low as 70-80K.

b. Practical pulse tube refrigerators can be designed and built by starting with an initial cut and try design, and using the tools developed in this effort to support local modeling and optimization to develop the final design.

Potential commercial applications include:

a. Long lifetime remote sensing applications.

b. Cryocoolers for Magnetic Imaging and Magnetic Resonance Imaging Systems where the very low vibrational and magnetic signatures of the pulse tube cryocooler are desirable.

c. Simple, high efficiency, high reliability pulse tube refrigerators have the potential to replace current Split-Stirling cryocoolers in numerous applications in space, military, scientific, and commercial applications.

PREPARED BY: DR. JOHN B. HENDRICKS, PRINCIPAL INVESTIGATOR
DR. MYRON E. CALKINS, PROJECT SCIENTIST
ALABAMA CRYOGENIC ENGINEERING, INC., (205) 536-8629
P.O. BOX 2470, HUNTSVILLE, AL 35804

TABLE OF CONTENTS

1.0 INTRODUCTION

The principal objective of this effort was:

> "The demonstration of a 0.25 Watt, 80 Kelvin Orifice Pulse Tube Refrigerator."

The program has been successful in meeting this objective. As discussed, an Orifice Pulse Tube Refrigerator has been demonstrated that reaches an ultimate temperature of 77 K, provides 1 Watt of cooling power at 97 K and is estimated to provide 0.2 W of cooling power at 80 K. It does so with a net electrical efficiency greater than previous versions of the Orifice Pulse Tube, as shown in figure 1.0-1.

In achieving this success, the analytical and experimental tasks have been strongly driven by experimental necessity and results. Early progress was attributable more to cut-and-try experimental approaches than to analytical design. Design and analysis tools existing at the beginning of the effort proved grossly unequal to the task of establishing an acceptable a-priori design. New analysis and design tools have been developed as an outgrowth of experimental success. These tools do not yet provide fully analytic design capability, but have been demonstrated to support local optimization of substantially acceptable baseline designs.

A secondary objective of the program was to produce a prototype Orifice Pulse Tube Refrigerator that conformed to the envelop of the "standard" Split-Sterling refrigerator(CTI-Cryogenics model CM-5). This objective was

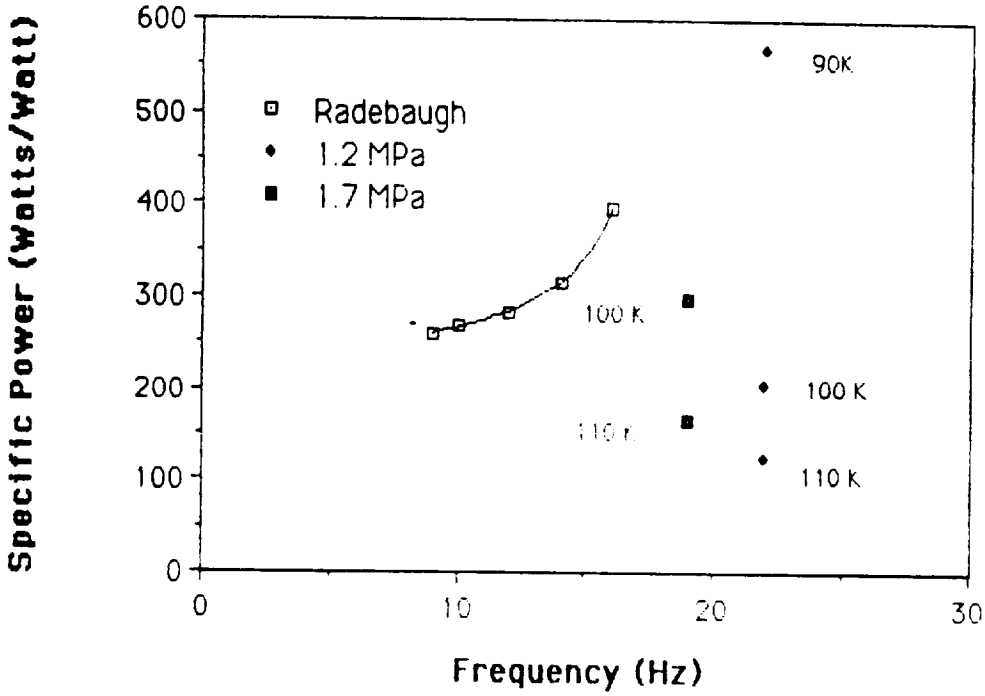

Figure 1.0-1. Specific power as a function of operating frequency for several different pulse tube cryocoolers. The data from Radebaugh (continuous curve) are for a temperature of 80K, and a pressure of 2 MPa. The isolated points are for the present effort. The points at 19 Hz are at a pressure of 1.7 MPa, those at 22 Hz are at a pressure of 1.2 MPa. Temperatures at which these levels of performance are achieved are indicated on the graph.

not met. The initial rationale for the effort to build a pulse tube within the Split-Stirling envelop was that although the pulse tube offers better reliability than the Stirling cycle systems, it was not expected to have as high a coefficient of performance, and the replacement of Stirling systems would be based primarily of a power/reliability tradeoff. Estimates of the volume efficiency of the pulse tube system indicate that it may actually be impossible to develop a unit to fit within the Stirling envelop, since (as discussed in section 2.2), the pulse tube is constrained to operate at lower pressure ratios than the Stirling cycle machines, and makes less effective use of the average mass flow. However, present data indicates that the specific power consumption of the current prototype rivals that of the Stirling, justifying a trade of the larger volume requirements of the pulse tube refrigerator against the lower reliability of the Stirling cycle machines.

This report is divided into five sections. The remainder of the introduction provides a short background discussion of the pulse tube. The second section details analytical and experimental progress and results. The third section describes the current experimental prototype. Conclusions are presented in the fourth section, and recommendations in the fifth.

1.1 Introduction to Pulse Tube Refrigerators

An excellent recent review of the status of research on pulse tube refrigerators is provided by Radebaugh (1990). This introduction borrows heavily from that source. Pulse tubes were first developed by Gifford and Longsworth (1963), and presently exist in three variants, the basic pulse tube, the resonant pulse tube, and the orifice pulse tube used in the present

effort. A fourth recent variant, the double inlet pulse tube has been reported by Shaowei, et.al. (1990). An excellent comparison of all the pulse tube types except the double inlet pulse tube is provided by Radebaugh (1986).

As shown in figure 1.1-1, all pulse tubes rely on the periodic compression of gas in a hollow tube connected to a regenerator. In addition, the orifice pulse tube has an orifice and associated orifice volume at the warm end of the pulse tube, while the double inlet pulse tube has additional valving and what amounts (in one form or another) to a phase shifting network between the compressor and the warm end of the pulse tube.

The basic pulse tube (Longsworth, 1967) operates at frequencies well below the resonant frequency of the tube, and appears to be limited to temperatures above about 120K. The resonant pulse tube (Wheatley, 1985) operates at the resonant frequency of the tube, and has reached temperatures as low as 195K. The orifice pulse tube was developed by Mikulin et. al. (1984) and has reached an ultimate temperature of 49K (Jintao Liang, et al., 1990).

The thermodynamic cycle of the pulse tube may be thought of (very approximately) as the midpoint between an adiabatic Ericsson and an adiabatic Stirling cycle. Compression and expansion are approximately adiabatic while heat absorption and rejection occur in the realm between constant pressure and constant volume (see section 2.2 for more details).

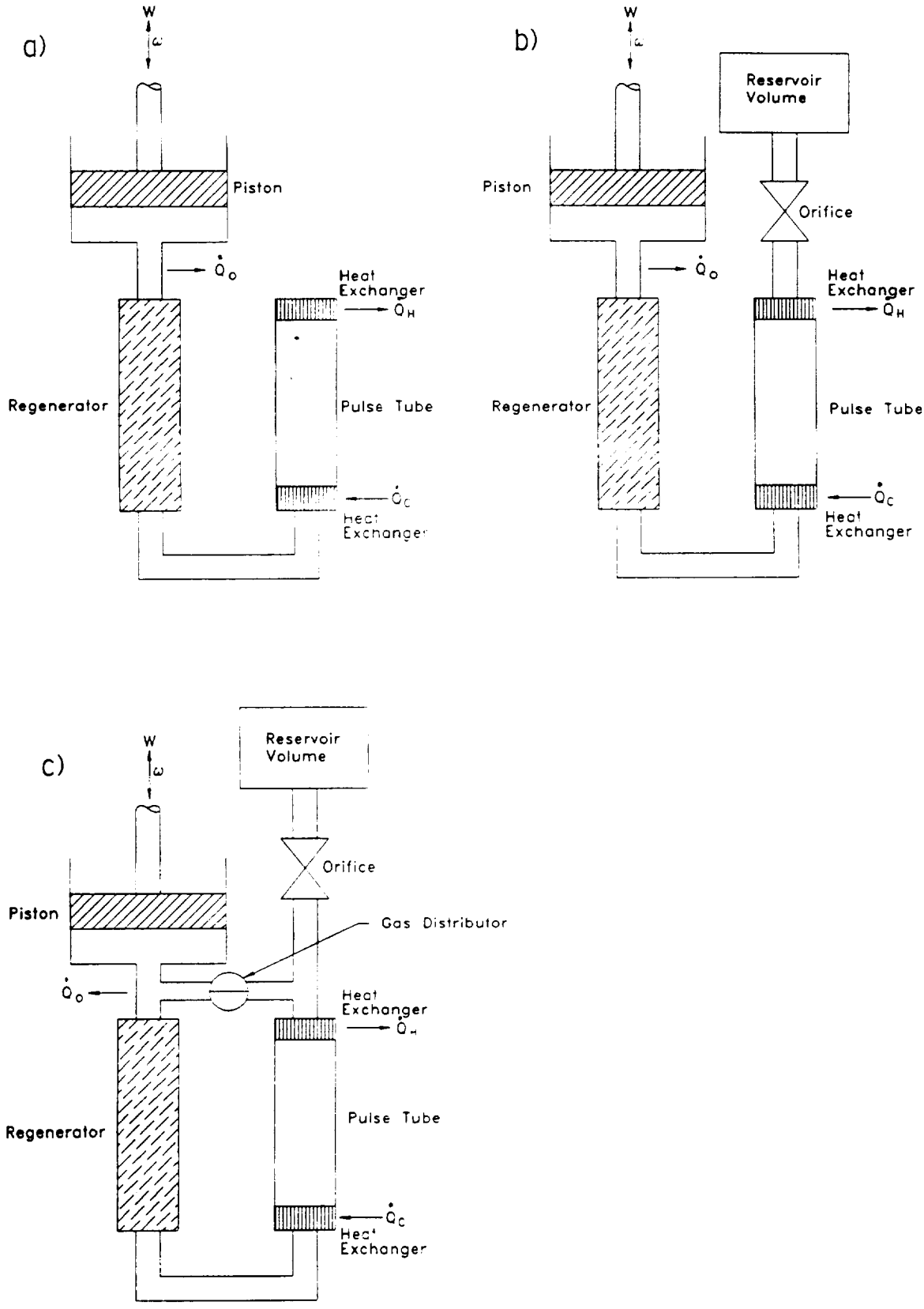

Figure 1.1-1 Three types of pulse tube refrigerator; a) basic pulse tube b) orifice pulse tube, and c) double inlet pulse tube.

1.2 Overview of Analytical Progress

At the beginning of the present effort, the analytical models of the pulse tube refrigerator, the pulse tube itself, and the regenerator were those presented in the proposal. These models were believed to provide an adequate theoretical and predictive framework to develop a-priori designs of acceptable pulse tubes. This proved to be wrong. Although the models provided some insight into the operation of the pulse tube, they did not permit a-priori design, and did not permit even local optimization of existing designs.

To replace these inadequate models, further analytical development was required. In the case of the system model, it was found that a very simple and straightforward model was sufficient to predict pressure ratios and mass flows accurately enough to drive the more detailed models of the regenerator and pulse tube that were also developed.

The model of the pulse tube that emerged was "Generalized Analysis", and is based on a correction and extension of existing work by Rallis, and extended by Walker (1979), and further discussed in the book (Walker, 1983). This model provides performance estimates for pulse tubes themselves, based on the working fluid, the pressure ratio R_p, the heating loads, and the efficiency of the regenerator. This model appears to be strictly accurate only in the limit of a zero dead-volume regenerator, and because of this, its utility remains limited to local optimization of existing designs, as discussed in section 2.4.

The regenerators used, whether parallel perforated plate or screen, fall loosely into the third category identified by Walker (1983), namely that the thermal conductivity of the matrix is effectively infinite normal to the fluid flow, and zero parallel to the flow. From that point on, each and every characteristic of the regenerator conspires to make analytical treatment intractable.

The principal difficulties with the required regenerator model include:

a. the materials properties are not independent of temperature,
b. the fluid inlet temperatures are constant neither in time nor in the flow section,
c. the heat transfer coefficients are constant neither in time nor along the passages,
d. the rate of mass flow is not constant during the blow.

Since these are precisely the opposite of the four requirements that Walker lists for tractable analysis, it is not surprising that the treatment by traditional methods is ineffectual.

We have adopted an approach that assumes a linear temperature gradient across the regenerator, and have applied the familiar tools of heat exchanger analysis. This approach is partially justified by noting that the regenerator dead volumes are a significant fraction of the total system volume, and that some of the fluid does not traverse the regenerator, but simply moves back and forth across portions of it. Examination of the work of Kays and London (1985) also shows that this approach results in a conservative design, as

discussed in section 2.3. A similar result appears in Nusselt's (Jakob, 1957) treatment of a regenerator with infinitely quick reversals of flow. This case reduces to that of a heat exchanger in which the two (inlet and return) fluids flow continuously, separated by metal walls.

The analytical approach taken provides a simple and tractable model that again appears to provide adequate guidance for local optimization but does not, in its present form, allow adequate a-priori designs.

As a result of the cut-and-try method adopted during the early experimental effort, sufficient experience has been accumulated with these models to instill a fair degree of confidence in their predictions. As long as the major parameters (pressure ratio, distribution of dead volume and mass flows) of the pulse tube system do not change too much, the models have proved qualitatively and quantitatively reliable for optimization. The design of the final series of regenerators in the experimental effort was guided by the use of these models, with excellent results.

1.3 Overview of Experimental Progress

The early experimental efforts in this program centered on the construction of the regenerator test facility and the pulse tube test facility. The regenerator test facility was completed and used to "bench" test early regenerator designs used in the experimental program. The pulse tube test facility was completed, and the experimental focus shifted to the design, construction, and test of a series of complete regenerator/pulse tube systems.

The initial design of the pulse tube test facility was found to be poorly suited to the experimental needs of the program. The major difficulty was created by the poor displacement match between the compressor (290cc) and the pulse tube systems (15-30cc). This mismatch resulted in the thermal dissipation of up to 5600 Watts in the compressor cylinder and gas handling panel, and associated dead volumes. The delivered gas was well above 300K and even a 2-stage heat exchanger was unable to absorb the load effectively. Although a number of experiments were conducted using the original facility, the lowest temperature reached was 102K for a pulse tube 1.27 cm in diameter and 24 cm long and a regenerator 2.5 cm in diameter and 7 cm long, filled with 700 stainless steel 400 mesh screens.

To permit a better displacement match, two 21cc compressors were acquired. A GAST model 1HAB-19 (1800 rpm dc powered) and the matching (1725 rpm) AC powered model. These compressors were encapsulated in pressure vessels to remove the forces associated with the average pressure in the system, the valves were removed to convert them to pressure wave generators, and they were mounted in the immediate vicinity of the cryostat, as discussed in section 2.4. The gas handling panel for the original pulse tube test facility continued to be used for charging and evacuating the pulse tube system. With the addition of these new compressors, thermal dissipation was greatly reduced, and easily controlled with a single 6 inch length of concentric tube heat exchanger installed in the middle of the connecting line running from the compressor to the top plate of the cryostat. Gas delivery temperature with tap water circulating in the exchanger was ~305K, and proved adequate for further experiments.

With this much simplified connection between the compressor and cryostat, rapid progress was made. A series of five different pulse tubes were constructed and tested using a single regenerator 0.95 cm OD and 13cm long containing 120 perforated copper plates 0.89 cm in diameter with 3800 95 micron holes. The results were in good local agreement with generalized analysis, and the best pulse tube was selected for use in optimizing the regenerator.

The analysis of the regenerator indicated that in order to maintain adequate wall-to-fluid contact at the cold end of the regenerator, a finer mesh screen was required. However, the model also showed that the use of smaller mesh at the upper (warm) end of the regenerator would introduce intolerable pressure drops across the regenerator, reducing the pressure ratio, and contributing to localized heating in the upper end of the regenerator. Using the regenerator analysis tools, several graded screen regenerators were designed. The current best effort prototype was constructed using a six stage graded screen regenerator with a measured efficiency (in run) of 98.5-99% and has reached a temperature of 77 K and provides a cooling power of 1 Watt at 97 K. These results are in good local agreement with generalized analysis and with the regenerator analysis/design techniques, as discussed in detail in section 2.4

2.0 THEORETICAL AND EXPERIMENTAL STUDIES

The four subsections describe the theoretical and experimental studies and progress in the following areas:

a) pulse tube refrigerator system model
b) pulse tube model (generalized analysis)
c) regenerator design and modeling tools
d) laboratory experiments and prototypes

The theoretical models presented here have been strongly driven by experimental results and requirements. They have also been used to guide the partial optimization that resulted in the current prototype.

2.1 Compressor and System Model

The system model connects all of the individual components of the pulse tube system, as shown in figure 2.1-1. The primary purpose of the system model is to support the calculation of pressure ratios and mass flows throughout the elements of the pulse tube cryocooler.

Throughout the discussion of the system model, we will follow the specific example shown in figure 2.1-1. Each of the components is described within the figure, and the relevant pressure ratios and mass flows are also shown.

Pressure Wave Generator. The purpose of the pressure wave generator is to generate a periodic pressure variation that, in turn, drives a periodic mass

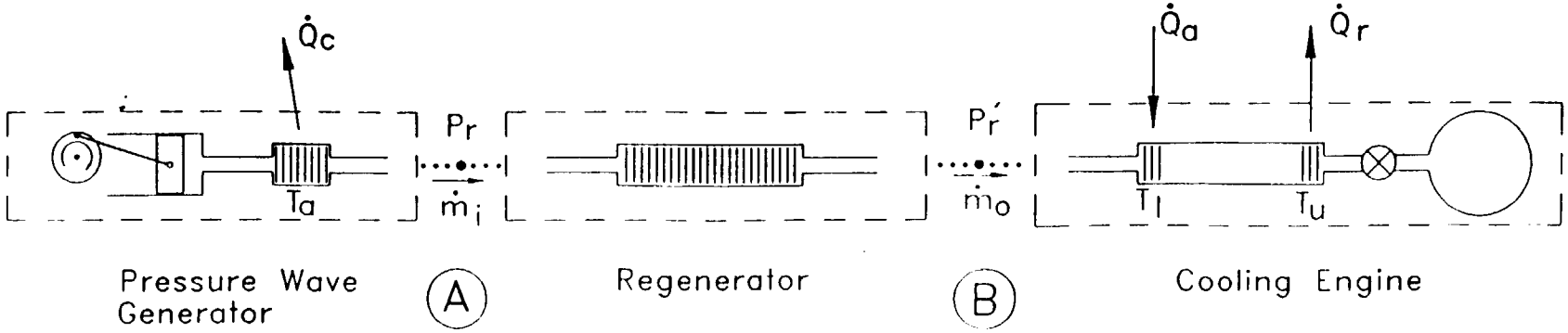

Pressure Wave Generator
- Effective displacement: 17.5 cc
- Frequency 12-30 Hz

Upper Connecting Line (compressor -> regenerator)

OD:	1/4 inch (0.635 cm)
ID:	0.186 inch (0.472 cm)
Length:	14.75 inch (37.5cm)
Volume:	6.57 cc

6 inch concentric tube heat exchanger

Regenerator

OD:	1/2 inch (1.27 cm)
ID:	0.480 inch (1.22 cm)
Length:	12 cm active length
Dead Volume:	11.35 cc
Flow Smoother:	25 80-mesh copper
Screens:	60 100-mesh
	104 150-mesh
	128 200-mesh
	164 250-mesh
	188 325-mesh
	240 400-mesh

Lower Connecting Line

OD:	1/8 inch (0.318 cm)
ID:	0.061 inch (0.155 cm)
Length:	10 cm
Volume:	0.19 cc

Pulse Tube

OD:	3/8 inch (0.95 cm)
ID:	0.355 inch (0.90 cm)
Length:	11 cm active length
Volume:	8.2 cc
Heat Ex:	25 80-mesh copper

Orifice Volume

Volume:	500cc

Operating Conditions

T_u	305 K
T_l	77 K
f	25 Hz
$P_{average}$	1.2 Mpa
P_r	1.47
P_r'	1.28
$\dot{m}_i$	1.22 g/s
$\dot{m}_o$	0.57 g/s

Figure 2.1-1 Characteristics of the current "best effort" prototype.

flow within the system. There are two types of PWG, variable volume and variable pressure. The variable pressure PWG alternately connects the components of the cryocooler to a pair of pressure reservoirs at different pressures. The pressure ratio is determined by the pressure difference between the reservoirs, and this difference is maintained by a valved compressor operating between the reservoirs. The compressor used in the test apparatus is of the variable volume type (G.A.S.T. 1HAB-19 with the valves removed). Using the manufacturers data for the free air flow rate of the compressor vs. delivery pressure, and attributing the decrease at high pressure to leakage around the rings, we can express the "effective" displacement of the compressor as a function of the delivery pressure, as shown in figure 2.1-2. The delivery pressure can be associated with either $\Delta P_{average}$, or with ΔP_{peak}, as shown in figure 2.1-3. At low pressure swings, the association probably ought to be to $\Delta P_{average}$, and at higher pressure swings, ought to approach ΔP_{peak}. This association allows us to plot effective volume as a function of pressure ratio for the compressor, as shown in figure 2.1-4.

Connecting line. The connecting line serves as the connection between the compressor and the cryostat. The dead volume of the connecting line can also be used to tune the pressure ratio in the pulse tube. The design of the connecting line is complicated by the heating derived from the repeated quasi-adiabatic compression of the gas in the connecting line. The heating is proportional to the volume of the connecting line, favoring small diameter and short length. However, as discussed below, the pressure drop across the connecting line rises rapidly as the diameter is decreased, raising the pressure ratio and the heating (per unit mass) within the line. This problem

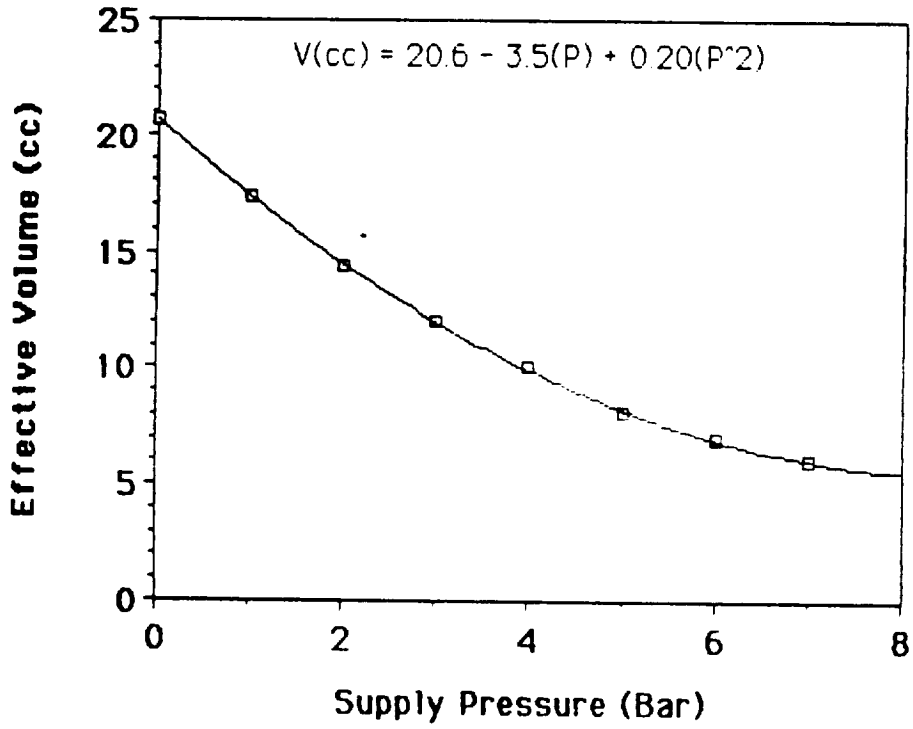

Figure 2.1-2 Effective volume vs. supply pressure (from manufacturers data).

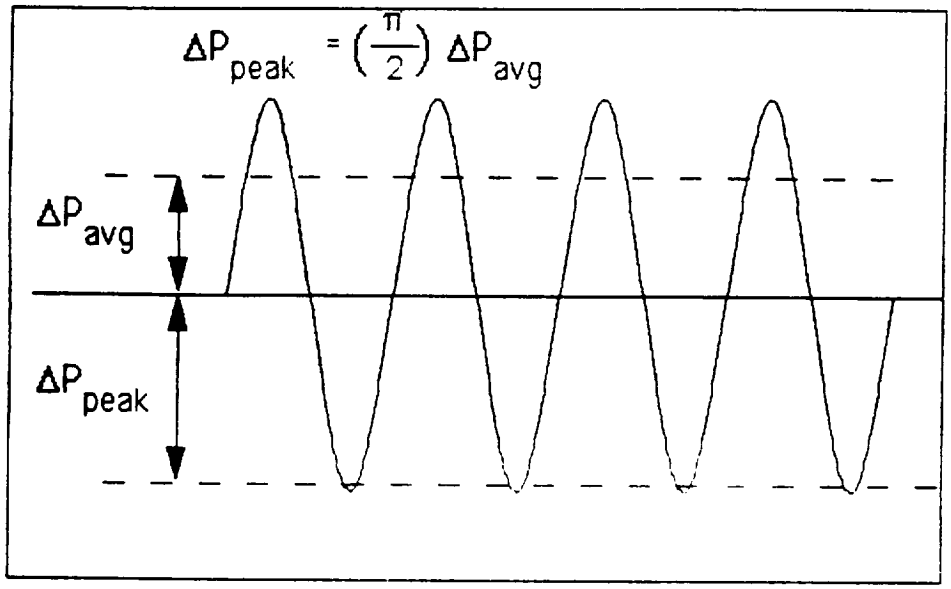

Figure 2.1-3 The definition and relationship between average and peak pressure swings.

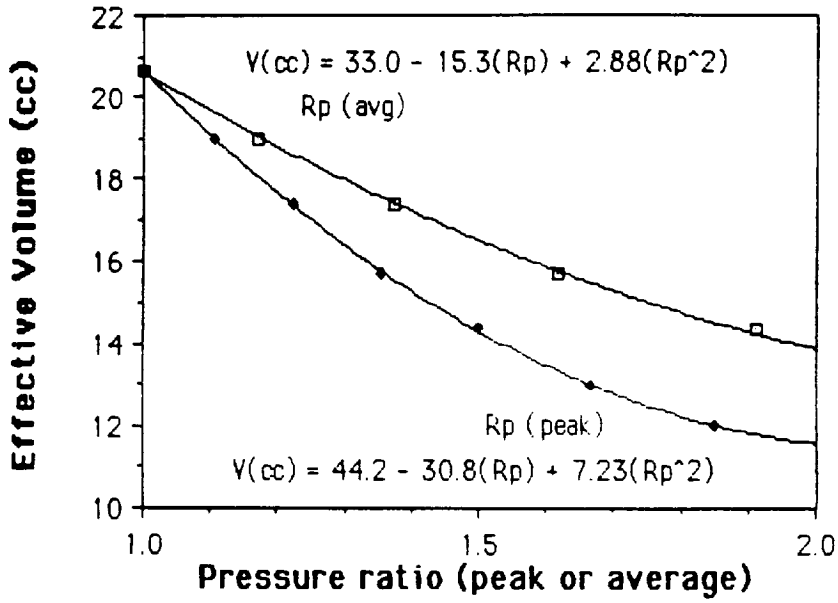

Figure 2.1-4 Effective volume vs pressure ratio.

has been encountered by other investigators, and the present line is a compromise between experimental convenience and theoretical perfection. The line in use has a total length of 37.5 cm and a diameter of 0.472 cm. A gas-water heat exchanger occupies the center 15 cm of the connecting line and carries away the heat generated in the line.

Regenerator. The regenerator is discussed extensively in the section on regenerator modeling (Sec 2.3) and in the experimental section (Sec 2.4). For the purposes of the system model, it is sufficient to note that the regenerator is the component with the largest dead volume and pressure drop, and that the regenerator supports a temperature gradient from room temperature on the upper (hot) end to the operating temperature (80K) on the lower (cold) end.

Pulse Tube. The pulse tube is discussed extensively in section 2.2. In the system model, it is represented as a dead volume supporting a temperature gradient identical to that across the regenerator.

Orifice and Orifice Volume. The orifice and orifice volume are treated below as part of the pulse tube. In the system model, the orifice and orifice volume contribute to the mass flow at the cold end of the pulse tube by allowing some of the warm gas to escape through the orifice during the compression stroke, and to return during the expansion stroke. The additional "effective" volume contributed to the pulse tube is included in the model of mass flow .

Pressure Ratio

One of the two primary functions of the system model is to predict the pressure ratio from the component characteristics. As discussed in the model of the pulse tube (Sec. 2.2), the performance of the pulse tube is a strong function of the pressure ratio at its opening. For the purposes of predicting the pressure ratio in the system, we use a simple model that accounts for the increase in density in the colder regions of the system. The temperature gradients across the pulse tube and the regenerator are broken into three regions. The lower (colder) third of the regenerator and pulse tube are taken to be at the lowest temperature, the middle third at the average temperature, and the upper third at room temperature. These average temperatures are used to compute the "effective" volume of that portion of the component. Using the current example, we have:

ROOM TEMPERATURE AND TEMPERATURE CORRECTED VOLUMES

T(upper) = 300K T(lower) = 80K

Component	V (cc) (room temp)	T (K) (running)	Eff. Volume (cc)
connecting line	6.57	300	6.57
regenerator (upper third)	3.78	300	3.78
regenerator (middle third)	3.78	190	5.97
regenerator (lower third)	3.78	80	14.19
lower conn. line	0.19	300	0.71
pulse tube upper end	0.60	300	0.60
pulse tube (upper third)	2.34	300	2.34
pulse tube (middle third)	2.34	190	3.69
pulse tube (lower third)	2.34	80	8.78
pulse tube lower end	0.60	80	2.25
Orifice line	6.90	300	6.90
TOTAL	33.22		54.78

For the simplest calculation, we assume that there are no pressure drops in the system and that the volumes may be considered lumped. In this case, the pressure ratio is given by:

$$R_p = R_v = [V_{max} / V_{min}] = [V_{compressor} + V_{tube}] / V_{tube}$$

For the case in point, using the graph of compressor effective volume vs pressure ratio (figure 2.1-4), we arrive at $R_p = 1.32$ and an effective volume of 17.5 cc for the compressor. The observed pressure ratio (measured at the warm end of the pulse tube) is $1.25 < R_p < 1.33$.

For more precise calculations of the pressure ratio and pressure ratio profile in the system, we resort to an electrical analog in which volumes are treated as capacitors and impedances are treated as resistors. This electrical analog is discussed below.

Mass Flow

Using the model for the pressure ratio, and again assuming that there are no pressure drops of consequence in the system, and that the temperature distribution in the system does not change substantially during the cycle, the average mass flow at each point in the system is given approximately by:

$$\langle \dot{m} \rangle = \frac{V_{DS}}{V_{tube}} \langle \dot{m}_c \rangle \qquad (2.1\text{-}1)$$

where V_{DS} is the "effective" volume "downstream" of the point at which the mass flow is measured. The average mass flow at the exit of the compressor $\langle \dot{m}_c \rangle$ is given by:

$$\langle \dot{m}_c \rangle = V_c \langle \rho \rangle (2f) \qquad (2.1\text{-}2)$$

In the example, 41.4cc of effective volume is downstream of the upper (hot) end of the regenerator. Therefore, the mass flow at this end of the regenerator is ~75% of $\langle \dot{m}_c \rangle$. At the cold end of the regenerator, only 32% of the effective volume remains downstream, and the mass flow at that end of the regenerator, and therefore in the cold end of the pulse tube is ~32% of $\langle \dot{m}_c \rangle$. Note that because of the large dead volume of the regenerator, ~40% of the mass flow from the compressor terminates in the regenerator, rather than in the pulse tube.

The simple model of mass flow is probably adequate for approximating the mass flow to/through the regenerator. The case is not so simple for the pulse tube. The temperature distribution in the pulse tube is believed to change during the cycle, and the mass flow at the cold end of the pulse tube is enhanced by the orifice at the hot end. There are four possible simple approaches:

a. use the simple model of mass flow with $V_{DS} = V_{pulse\ tube}$,
b. use the simple model of mass flow and include an additional 1/3 of the pulse tube volume in the calculation of effective volume downstream of the pulse tube entrance
c. treat the compression of the gas in the pulse tube as an adiabatic process, compute the change in gas volume, note that this volume change is filled by cold gas from the cold end of the regenerator, and correct the volume to room temperature using the temperature ratio

d. treat the compression of the gas in the pulse tube as isothermal and again correct the volume change for the temperature ratio.

These approaches predict:

a. 32% of $\langle \dot{m}_c \rangle$

b. 36.5% of $\langle \dot{m}_c \rangle$

c. 25% of $\langle \dot{m}_c \rangle$

d. 44% of $\langle \dot{m}_c \rangle$.

The actual process in the pulse tube lies between the adiabatic and isothermal extremes, encouraging us simply to average the two estimates, giving 34.5%, which in turn is near the predictions from (a) and (b). A good estimate for the mass flow in the example is therefore ~35% $\langle \dot{m}_c \rangle$.

Pressure Drops

As discussed, the simple models above assume that there are no significant pressure drops in the system. This assumption is not as restrictive as it seems, since any pressure drop results in localized heating, and reduces the final pressure ratio in the pulse tube, reducing performance. We will examine the pressure drops generated by each of the elements of the current prototype pulse tube cooler.

Three elements of the pulse tube system can generate significant pressure drops:

a. the upper connecting line (from compressor to regenerator),

b. the lower connecting line (from regenerator to pulse tube),

c. the regenerator.

We have examined the pressure drops in each of these components using incompressible fluid mechanics. Levenspiel (1984) states that for pressure ratios less than ~2, incompressible and compressible calculations will give approximately the same answer. In normal operation, and in the example case here, the upper connecting line is in fully turbulent flow, while the regenerator and lower connecting line are in laminar flow, as discussed below.

Connecting lines. For flow in a smooth pipe, the Reynolds number is given by (Incropera, 1985)

$$Re_D = \frac{\rho \mu_m D}{\mu} \qquad (2.1\text{-}3)$$

where ρ is the density, μ_m the average fluid velocity, D the diameter and μ the viscosity. For the example taken here, the Reynolds number in the upper connecting line is about 30,000 for the average mass flow and about 47,000 for the peak mass flow. Clearly, the upper connecting line is in turbulent flow, and the friction factor is given by (Incropera, 1985):

$$f = 0.316\ Re_D^{-1/4} \qquad Re_D \leq 2x10^4 \qquad (2.1\text{-}4)$$

$$f = 0.184\ Re_D^{-1/5} \qquad Re_D \geq 2x10^4 \qquad (2.1\text{-}5)$$

with

$$\Delta P = \frac{f \rho\ u_m^2\ L}{2D} \qquad (2.1\text{-}6)$$

Substituting the expression for the Reynolds number (2.1-3) into (2.1-4) and (2.1-5) and expressing the result in terms of the mass flow and connecting line diameter, we get:

$$\Delta P = 0.241 \frac{\dot{m}^{3/4} \mu^{1/4} L}{\rho D^{15/4}} \qquad Re_p \leq 2x10^4 \qquad (2.1\text{-}7)$$

$$\Delta P = 0.142 \frac{\dot{m}^{9/5} \mu^{1/5} L}{\rho D^{24/5}} \qquad Re_D > 2x10^4 \qquad (2.1\text{-}8)$$

The pressure drop in the upper connecting line is approximately 10,000 Pa, which is negligible compared to the 150,000 Pa periodic pressure swing in the pulse tube.

Similarly, the Reynolds number and pressure drop can be calculated for the lower connecting line. The flow is found to be turbulent, and the pressure drop is less than 25,000 Pa. Again, this is small relative to the periodic pressure swing at that point in the system.

The pressure drop in the graded regenerator is somewhat harder to calculate. The regenerator is broken into six sections corresponding to the different mesh screens, the temperature gradient across the regenerator is taken to be linear, and the pressure drop in each section is calculated using the average temperature and mass flow in that section. The results are shown in figure 2.1-5.

The computations were performed using the hydraulic diameter of the approximately square holes in the screens, and treating the stacked screens as

tup	300 K
tlo	80 K
tlen	12 cm
den300	1.61 kg/m**3
tubdia	0.46 in
mdotup	1.22 g/s
mdotlo	0.57 g/s
pbar	1.00E+06 n/m**2
rp	1.25
deltap	111111 n/m**2

mesh	100	150	200	250	325	400
wiredia	0.0045	0.0036	0.0021	0.0018	0.0014	0.0011
mdot	1.11	1.00	0.90	0.79	0.68	0.57
Length	2.00	2.00	2.00	2.00	2.00	2.00
sumlen	2.00	4.00	6.00	8.00	10.00	12.00
T	281.67	245.00	208.33	171.67	135.00	98.33
den	1.71	1.97	2.32	2.81	3.58	4.91
vis	1.91E-05	1.72E-05	1.53E-05	1.34E-05	1.15E-05	9.57E-06
nhole	1662	3739	6648	10387	17554	26590
hyddia	1.40E-04	1.03E-04	7.37E-05	5.59E-05	4.26E-05	3.56E-05
hydarea	1.53E-08	8.38E-09	4.26E-09	2.45E-09	1.42E-09	9.93E-10
area	1.95E-08	1.07E-08	5.43E-09	3.12E-09	1.81E-09	1.26E-09
totalhydarea	2.55E-05	3.13E-05	2.83E-05	2.55E-05	2.50E-05	2.64E-05
totalarea	3.24E-05	3.99E-05	3.61E-05	3.24E-05	3.18E-05	3.36E-05
volrate	6.48E-04	5.09E-04	3.86E-04	2.80E-04	1.90E-04	1.16E-04
vel	19.99	12.76	10.70	8.62	5.95	3.45
reynolds	250.64	151.05	119.54	101.27	79.05	62.99
f	0.26	0.42	0.54	0.63	0.81	1.02
dpdx	626093	657946	965183	1182344	1205171	835860
pdrop	12522	13159	19304	23647	24103	16717

totalDrop	109452 n/m**2
DPpeak	270061 n/m**2

pswing	2.92E+05 n/m**2
rptop	1.82

Figure 2.1-5 Calculation of pressure drop in graded screen regenerator.

many continuous holes through that section of the regenerator, effectively turning the screens into perforated plates. This approximation is acceptable for Reynolds numbers less than about 100, and results in increasingly large errors for higher Reynolds numbers, as shown in figure 2.1-6, which is reproduced from page 149 of Kays and London. The computed values in figure 2.1-5 are approximately correct, since most of the pressure drop in the regenerator occurs on the cold (low Reynolds no.) end.

The values in figure 2.1-5 are for the most efficient graded screen regenerator used in the experiments. The measured pressure drops are not as large as those predicted in figure 2.1-5.

The Electrical Analog

In treating the effects of pressure drops on the pressure ratio, it is important to note that the maximum pressure drop in the regenerator coincides with the maximum local mass flow, while the maximum pressure coincides with the zeroes in the local mass flow. This means that the pressure drops cannot simply be used to correct the upper and lower pressures and recompute the pressure ratio.

The electrical analog is useful in treating this case. The pressure is associated with the voltage, the mass flow with the current, pressure drops with resistance, and dead volumes with capacitance. In the electrical case we have:

$$V = IR \qquad (2.1\text{-}9)$$

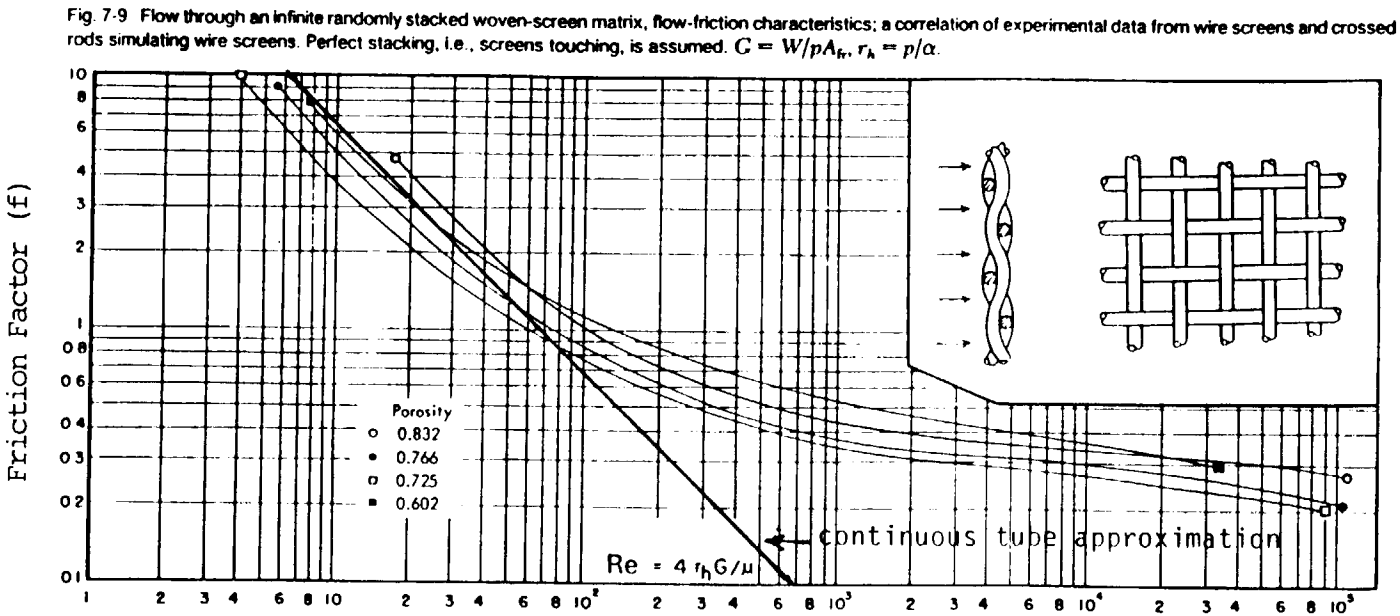

Figure 2.1-6 Friction factor for screens. Reproduced from Kays and London (1985), with the continuous tube approximation superimposed.

$$\frac{dV}{dt} = \frac{I}{C} \tag{2.1-10}$$

while for pressure and mass flow, we have:

$$\Delta P = \dot{m} \left(\frac{128\ \mu\ L}{\pi\ \rho\ D_h^4\ N_h}\right) \tag{2.1-11}$$

for the pressure drop across a screen or perforated plate with N_h holes of hydraulic diameter D_h. For the isothermal addition of mass to a fixed volume we have:

$$\frac{dP}{dt} = \dot{m} \left(\frac{RT}{m_o V}\right) \tag{2.1-12}$$

where m_o is the molar weight. The result of significance here is that the pressure swing ΔP and the pressure drop P_{drop} are 90^o out of phase and must be added in quadrature. The total pressure swing at the entrance to the regenerator (from which the pressure ratio is calculated) is given by

$$\Delta P_{entrance} = [P^2_{drop\text{-}regenerator} + \Delta P^2_{pulse\ tube}]^{1/2} \tag{2.1-13}$$

The pressure ratio predicted using addition-in-quadrature for the pressure swing in the pulse tube and the pressure drop across the regenerator is 1.82. The measured value is between 1.47 and 1.64, depending on the average pressure.

In summary, the simplified system model presented here provides rough estimates of pressure ratio and mass flow. These estimates are accurate enough to drive the generalized analysis model of the pulse tube, and the regenerator model.

2.2 Pulse Tube Model

In this section we will present a basic theory for the Orifice Pulse-Tube cryocooler. Two previous approaches to this problem include:

a. The surface heat-pumping approach of Gifford and Longsworth.
b. The enthalpy-flow approach of Radebaugh, et al.

Our approach will use basic cycle thermodynamics as a starting point. We will show that this approach reduces to the enthalpy-flow approach for optimized cycle conditions. Our approach will not answer the question, "How does an Orifice Pulse-Tube Cryocooler really work?". However, it will give the interrelation of the thermodynamic variables, and this is of primary importance to a cryocooler designer.

The testing program of Radebaugh at NIST has shown that the enthalpy-flow model of the orifice pulse-tube cryocooler accounted for the observed behavior. This was done in a test facility that was able to simulate ideal regeneration and pressure wave generation. Therefore, the functional relations in the enthalpy-flow model have been substantially confirmed. Thus, since the generalized analysis approach gives similar relations, it too has been confirmed. The surface heat-pumping approach appears to be more applicable to the "basic" pulse-tube. That is, a pulse-tube without an orifice and orifice volume.

2.2.1 Generalized Analysis

Generalized analysis was originally developed by Rallis, but has been extended by Walker. Both the original paper, Walker (1979) and the later version in the book, Walker (1983), include many errors in the equations. We have gone through this work, and corrected the errors, so that we can use the technique to analyze cryocoolers. The analysis considers two basic types of compression and expansion processes, isothermal and adiabatic. Two regeneration processes are also considered, constant volume and constant pressure. We have found that the constant pressure regeneration processes along with adiabatic compression and expansion processes seem to be reasonable choices to model the orifice pulse tube cryocooler. A short review of the generalized analysis will be given, and then it will be applied to the pulse-tube cryocooler.

A schematic of a generalized cryocooler is given in Figure 2.2.1-1. P-V and T-S diagrams for the generalized, adiabatic process with constant volume regeneration is shown in Figure 2.2.1-2. This cycle corresponds to an adiabatic Stirling machine. Definitions of the quantities used in the analysis are given in Table 2.2.1-1. The equations for $W/\dot{m}$, $\dot{Q}/\dot{m}$, and COP are included in the figure. A corresponding figure for a generalized, adiabatic process with constant pressure regeneration is shown in Figure 2.2.1-3. This cycle corresponds to an adiabatic Ericsson machine.

The equations for $\dot{Q}$ in the figures can be compared to the equivalent equation for $\dot{Q}$ developed by Radebaugh. Radebaugh used an enthalpy flow calculation to derive the refrigeration power. This required the use of phasor analysis to account for the phase shift induced by flow in the orifice. Generalized

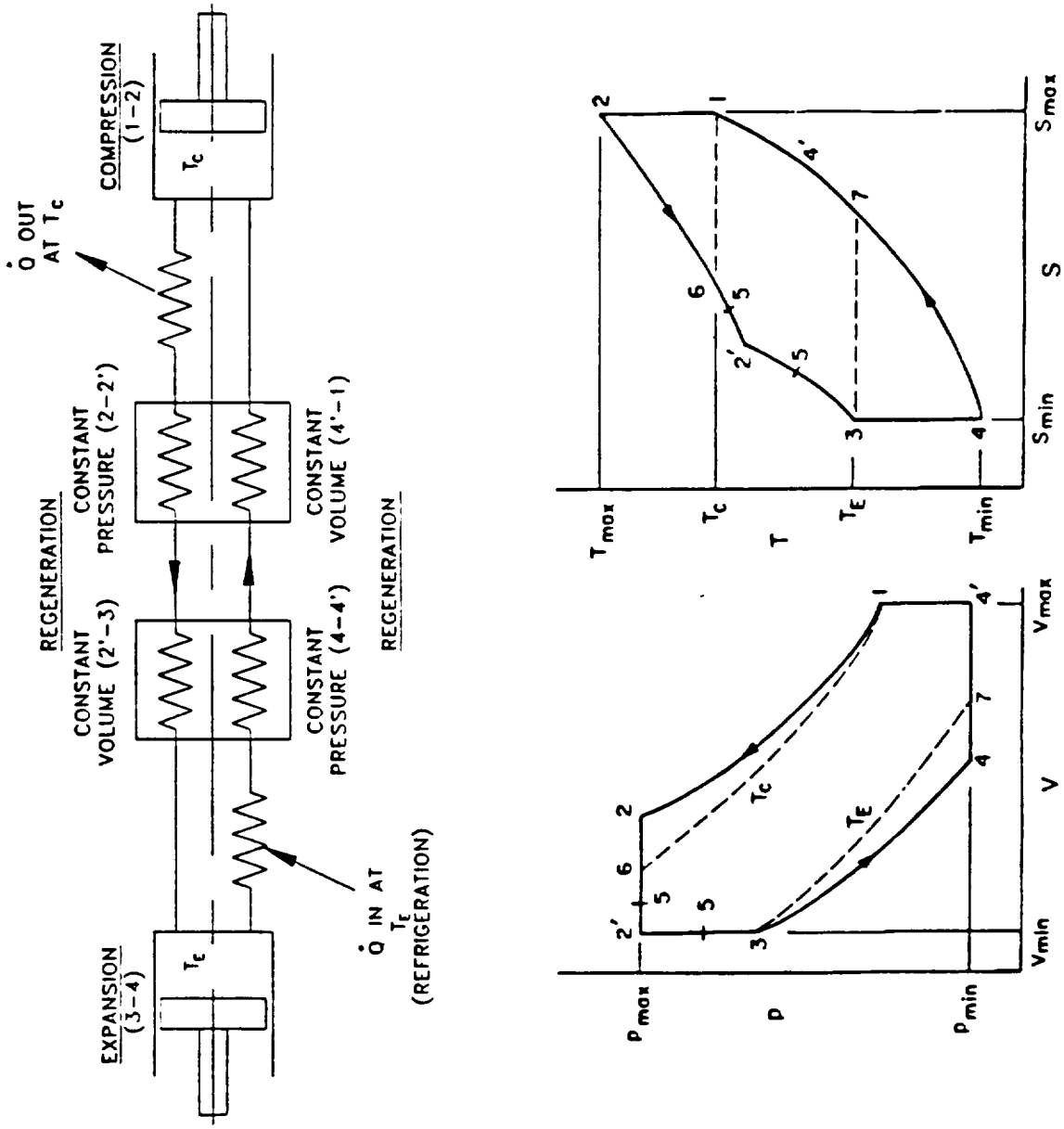

Figure 2.2.1-1 A Generalized Cryocooler Cycle with Adiabatic Expansion and Compression

$$W = RT_E(r^{\gamma-1}-1)(\tau r^{\gamma-1}-1)/[r^{\gamma-1}(\gamma-1)]$$

$$\dot{Q} = RT_E\,[1 - 1/r^{\gamma-1} - (\tau-1)(1-\epsilon)]/(\gamma-1)$$

$$COP = [r^{\gamma-1} - 1 - r^{\gamma-1}(\tau-1)(1-\epsilon)]/(r^{\gamma-1} - 1)(\tau\, r^{\gamma-1} - 1).$$

And with $\epsilon = 1$:

$$\dot{Q}_{(\epsilon=1)} = RT_E\,(1 - 1/r^{\gamma-1})/(\gamma-1)$$

$$COP_{(\epsilon=1)} = 1/(\tau r^{\gamma-1}-1)$$

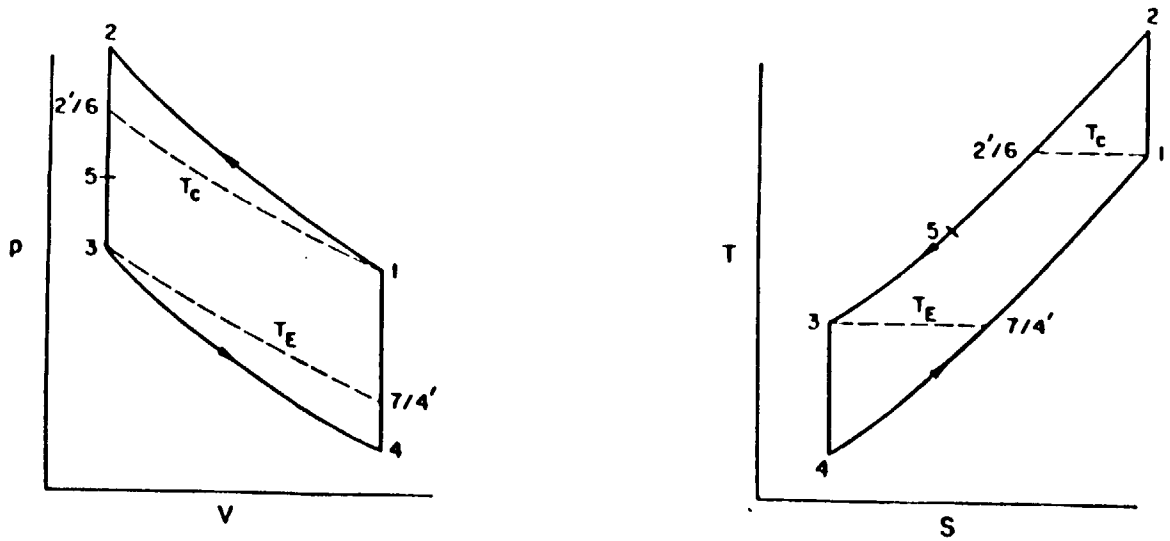

Figure 2.2.1-2 The Adiabatic Stirling Cycle

TABLE 2.2.1-1

Definition of Quantities for Generalized Analysis

r = volume expansion ratio

ϵ = regenerator effectiveness

τ = temperature ratio, T_C/T_E

T_C = compression temperature

T_E = expansion temperature

$\dot{Q}/\langle\dot{m}\rangle$ = specific cooling power at T_E

$W/\langle\dot{m}\rangle$ = specific work input at T_C

COP = coefficient of performance, $\dot{Q}/W$

γ = ratio of specific heat, c_p/c_v

$$W = RT_E\gamma(r^{\gamma-1}-1)(\tau r^{\gamma-1}-1)/[r^{\gamma-1}(\gamma-1)]$$

$$\dot{Q} = RT_E\gamma[1 - 1/r^{\gamma-1} - (\tau-1)(1-\epsilon)]/(\gamma-1)$$

$$COP = [r^{\gamma-1} - 1 - r^{\gamma-1}(\tau-1)(1-\epsilon)]/(r^{\gamma-1} - 1)(\tau\, r^{\gamma-1} - 1).$$

With $\epsilon = 1$ these become:

$$\dot{Q}_{(\epsilon=1)} = RT_E\gamma\,(1 - 1/r^{\gamma-1})/(\gamma-1)$$

$$COP_{(\epsilon=1)} = 1/(\tau r^{\gamma-1}-1)$$

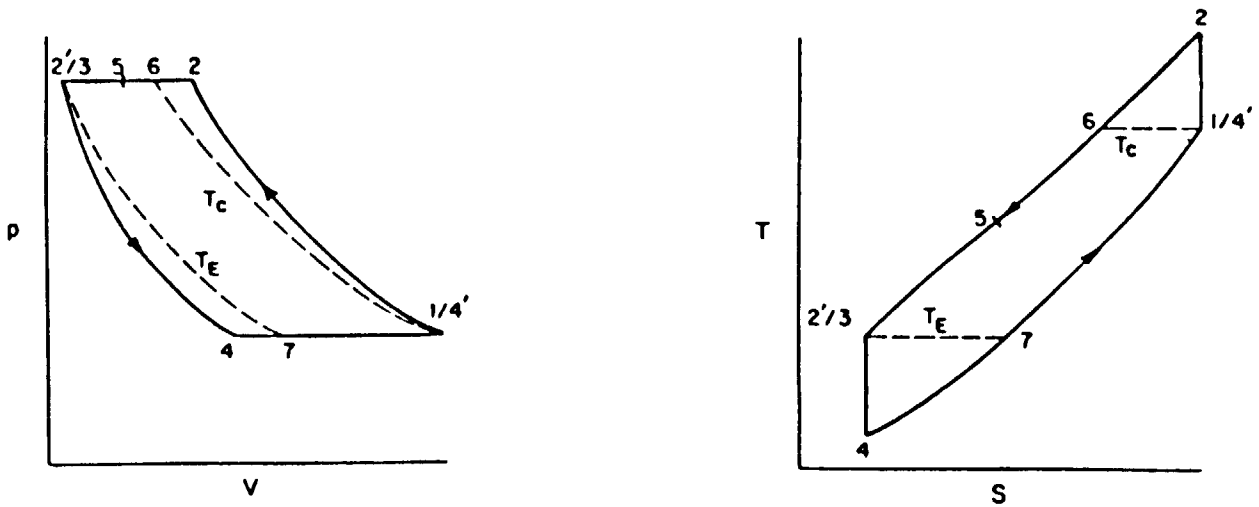

Figure 2.2.1-3 The Adiabatic Ericsson Cycle

analysis considers none of these detailed variables that are unique to the pulse tube. This leads to the first assumption.

Assumption #1: Generalized analysis predicts the maximum value for COP, $\dot{Q}$, W, etc. based on the available volume compression and expansion ratios, temperature ratio, regenerator effectiveness, and specific heat ratio of the working fluid. If the "internal" variables are not optimized, the values can be much less than the maximum values given by generalized analysis.

The equations given in Figures 2.2.1-1 and 2.2.1-3 were developed on the assumption that the volume compression ratio, r_c, was the same as the volume expansion ratio, r_e. We can then introduce a degradation factor, η_D, into the analysis in order to account for loss factors. Radebaugh carried out the same basic process, and found that the actual refrigeration power (by experiment) for the orifice pulse-tube cryocooler was 1/3 the power predicted by the enthalpy flow model. We can use the same factor in our analysis. Therefore

$$\dot{Q}_p = 1/3\ \dot{Q}_{ga} \qquad (2.2.1\text{-}1)$$

$$W_p = 1/3\ W_{ga} \qquad (2.2.1\text{-}2)$$

$$COP_p = \frac{\dot{Q}p}{Wp} = \frac{1/3\ \dot{Q}_{ga}}{1/3\ W_{ga}} \qquad (2.2.1\text{-}3)$$

where the p subscript corresponds to predicted values and the ga subscript corresponds to values obtained from generalized analysis.

Assumption #2: The pulse tube refrigerator does not have a well-defined volume expansion ratio like the typical cryocooler with a displacer or expander piston. Therefore, we will account for this difference in cycle operation by introducing a degradation factor, η_D. This factor should be constant with temperature, pressure ratio, etc. but might change for different ratios of compressor volume to pulse tube volume.

A series of charts have been developed to predict the COP and $\dot{Q}$ of the pulse tube cryocooler as a function of expansion ratio and temperature. Five charts (figs. 2.2.1-4 through 2.2.1-8) give COP vs. r at τ = 2, 3, 4, 5 & 6. Five charts (figs. 2.2.1-9 through 2.2.1-13) give $\dot{Q}$ vs. τ at r = 1.2, 1.4, 1.6, 1.8 and 2. Effectiveness is a parameter in both sets of charts. The ten charts for a series of "design" charts, and should allow us to predict the operation of a pulse-tube cryocooler under a variety of circumstances.

2.2.2 Application of Generalized Analysis to Pulse Tubes

The expansion and compression processes in the orifice pulse-tube cryocooler will be approximately adiabatic. The heat exchange and regeneration processes will be carried out in low pressure drop systems, that have a fixed volume. This means that the heat exchanger and regeneration processes are constant pressure. Therefore, we assume that orifice pulse-tube cryocooler operates on an Adiabatic Ericsson Generalized Cycle.

Some uses of the charts include:

a.) If we know the volume expansion ratio, r, we can determine the specific refrigeration power $\dot{Q}/\dot{m}$. Then, if we know the mass and specific

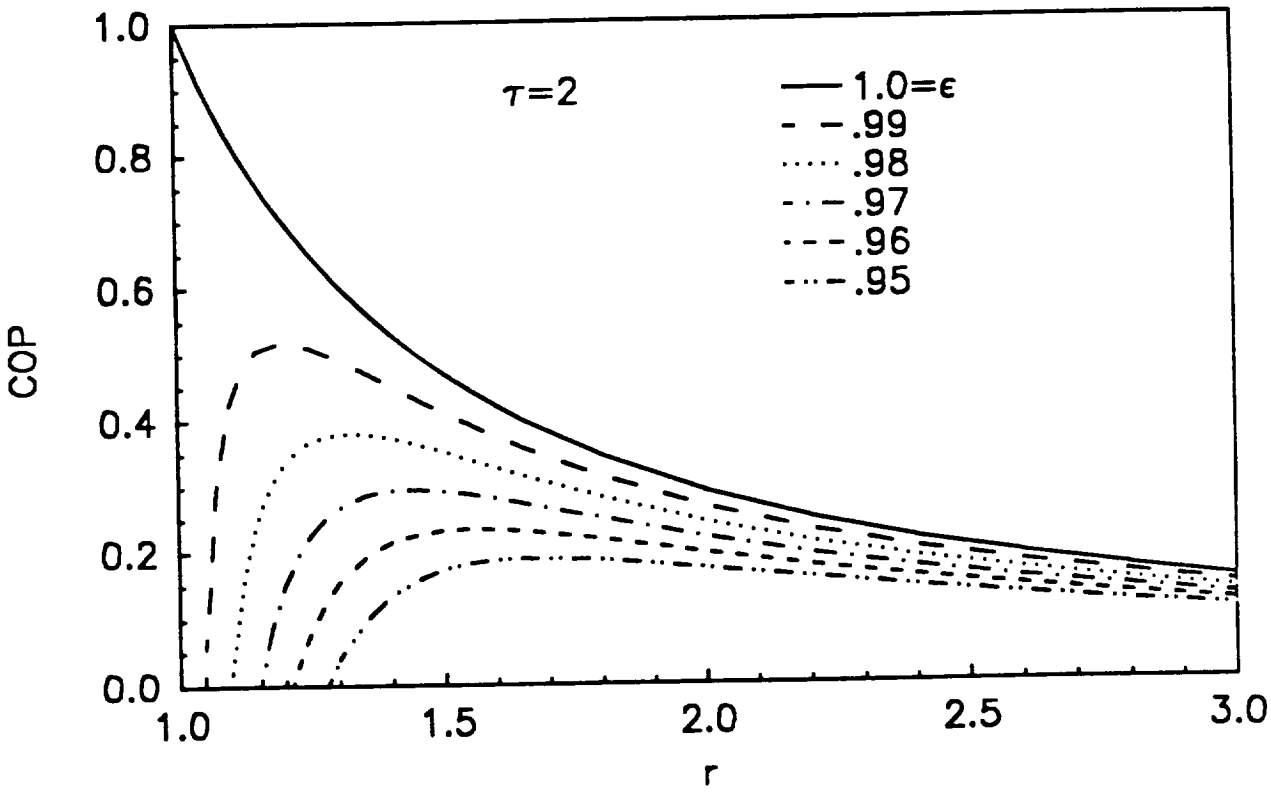

Figure 2.2.1-4 Coefficient of Performance of an Orifice Pulse-Tube as a Function of Expansion Ratio at $\tau=2$.

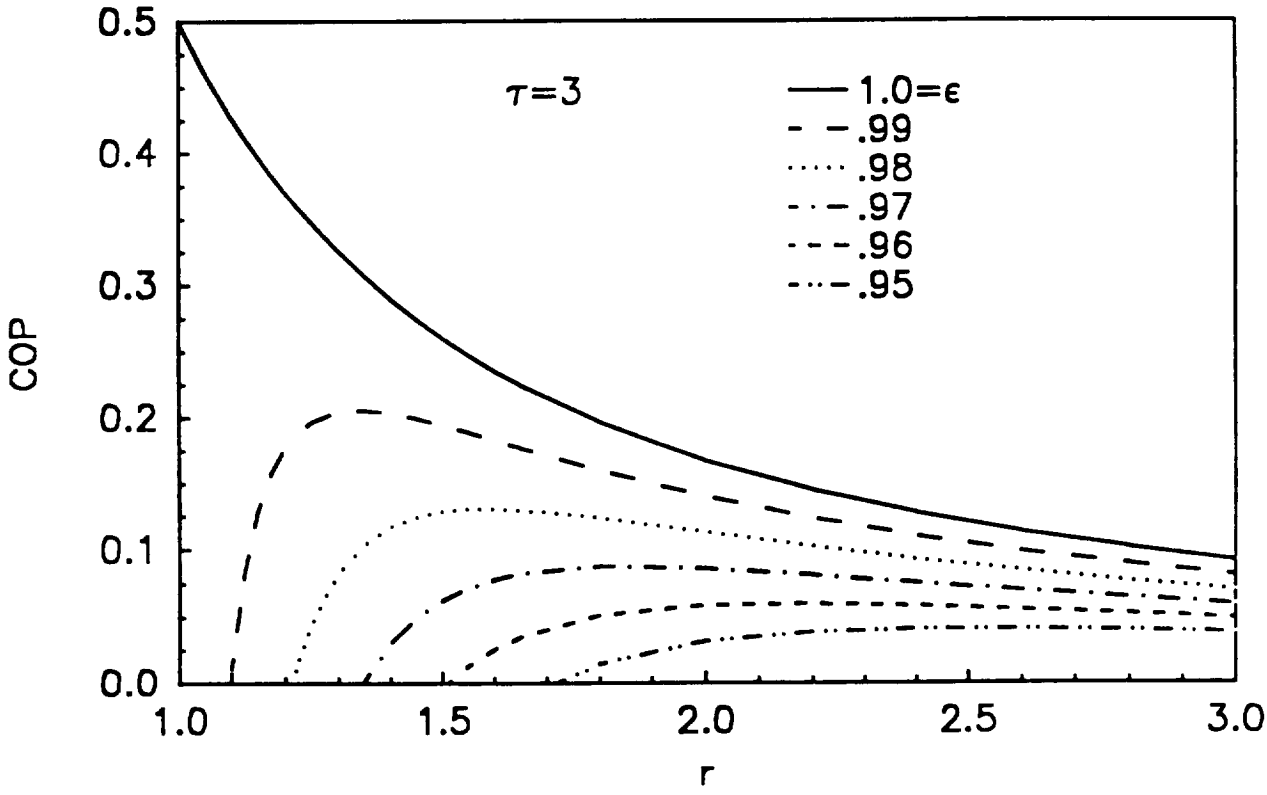

Figure 2.2.1-5 Coefficient of Performance of an Orifice Pulse Tube as a Function of Expansion Ratio at τ=3.

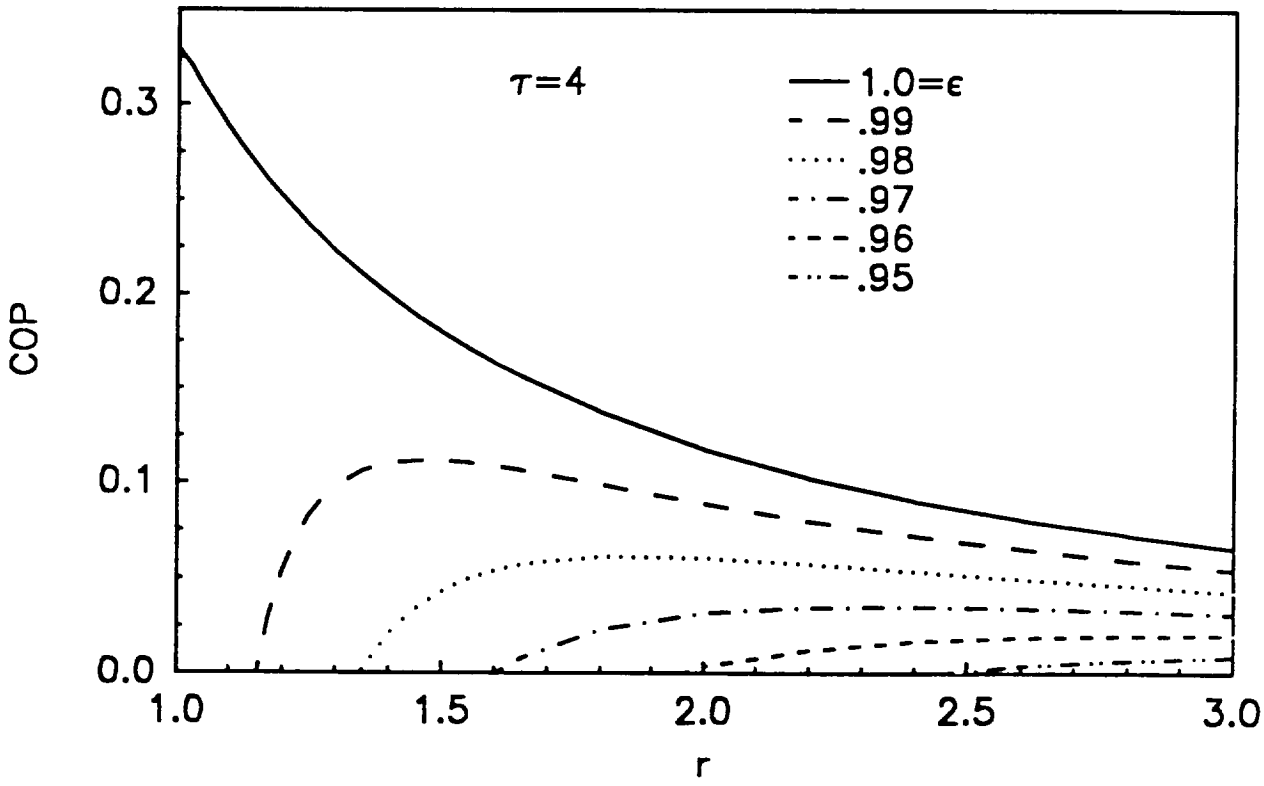

Figure 2.2.1-6 Coefficient of Performance of an Orifice Pulse-Tube as a Function of Expansion Ratio at τ=4.

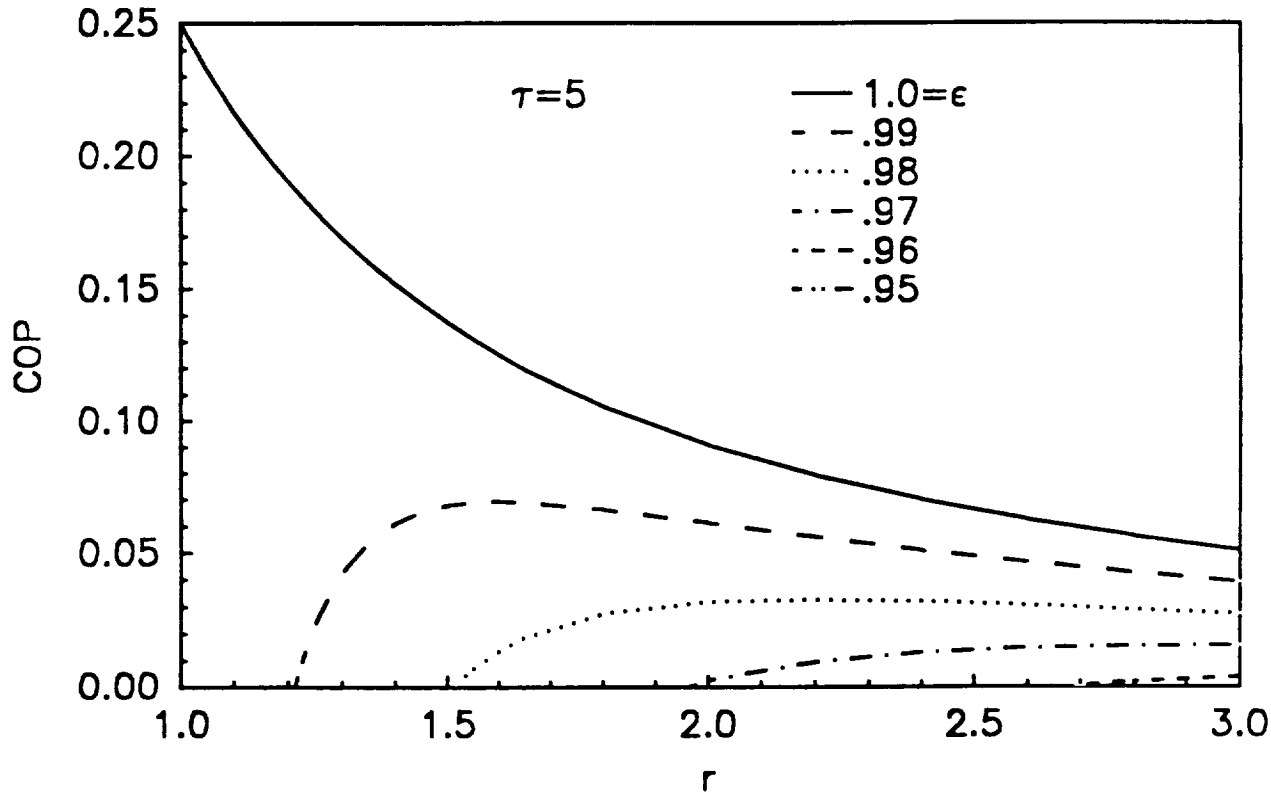

Figure 2.2.1-7 Coefficient of Performance of an Orifice Pulse-Tube as a Function of Expansion Ratio at τ=5.

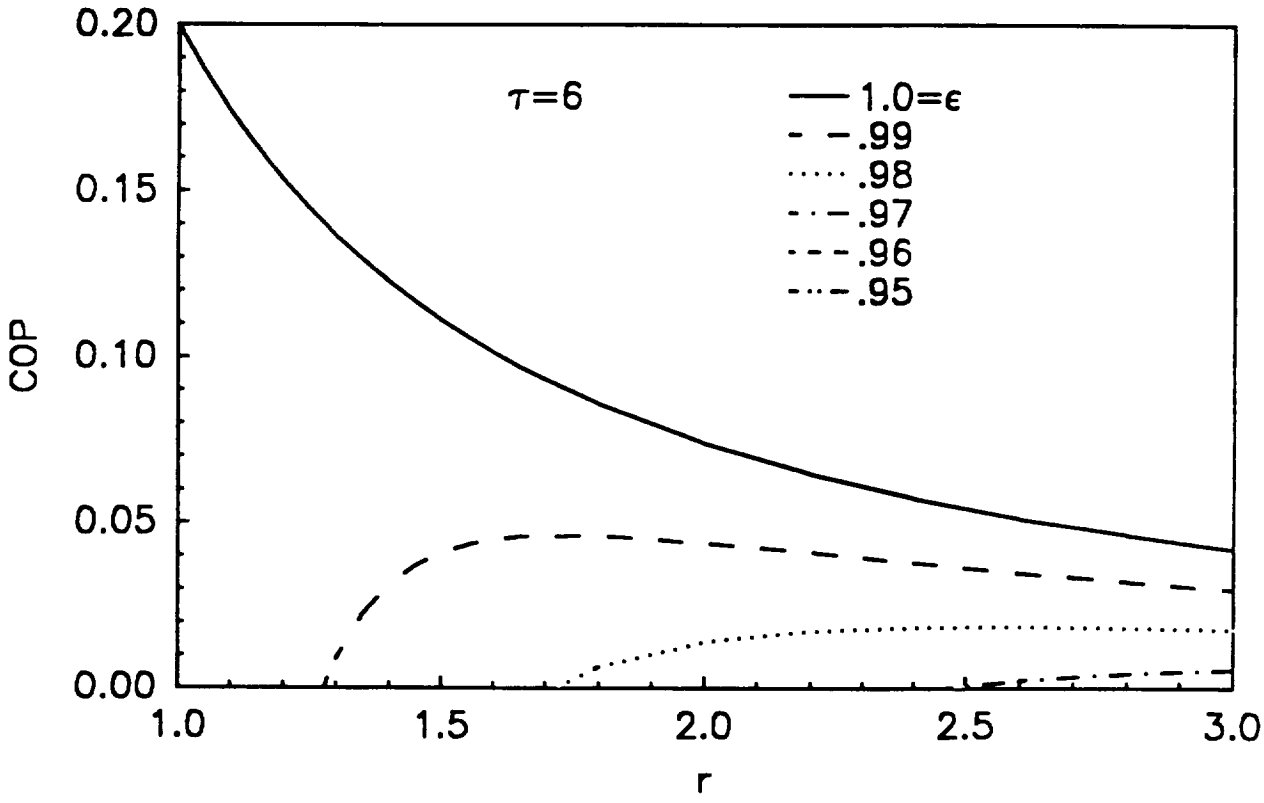

Figure 2.2.1-8 Coefficient of Performance of an Orifice Pulse-Tube as a Function of Expansion Ratio at τ=6.

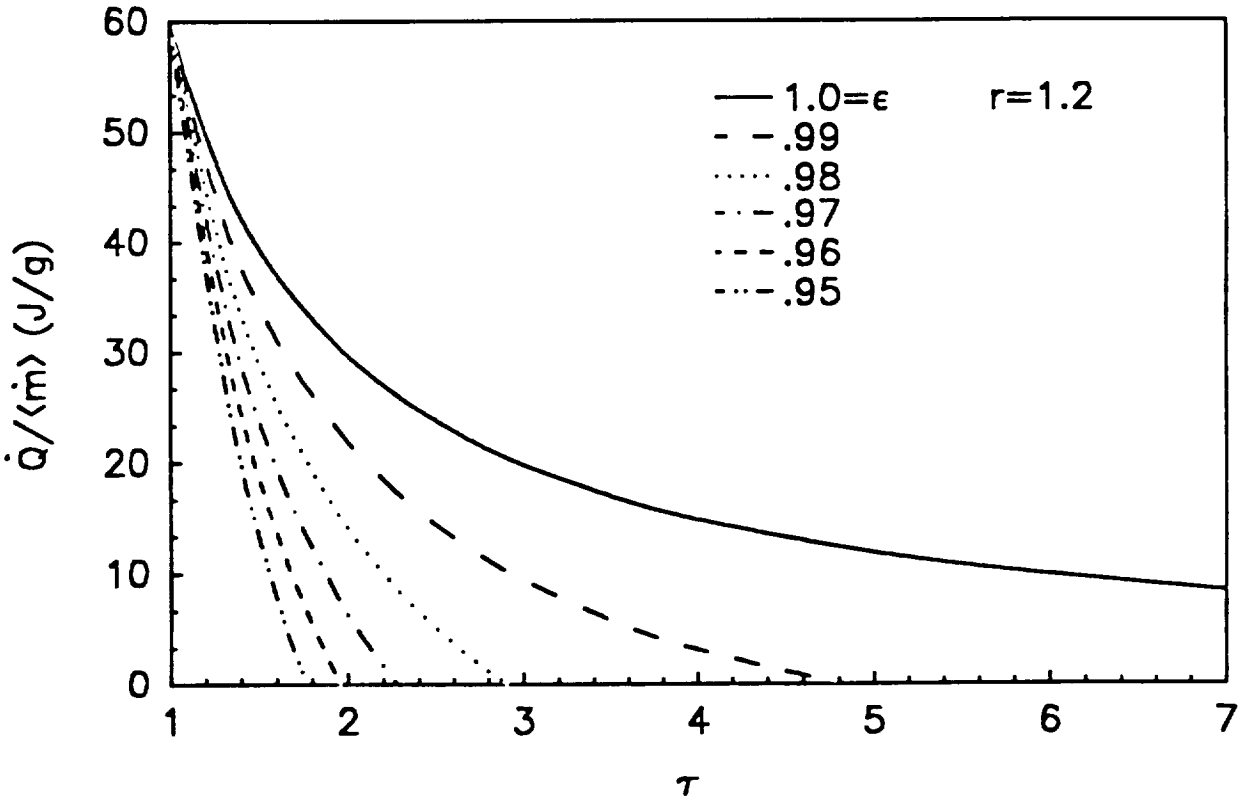

Figure 2.2.1-9 Specific cooling power as a function of temperature ratio for an expansion ratio, r=1.2.

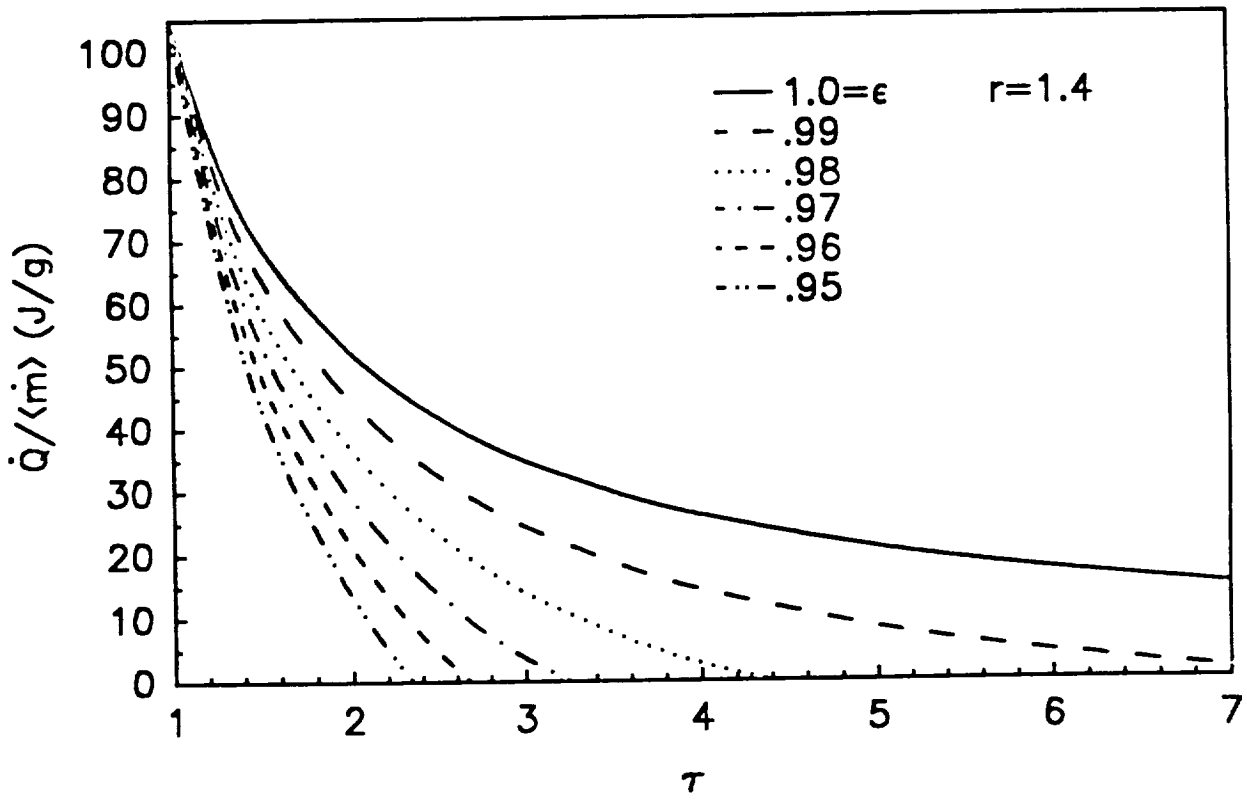

Figure 2.2.1-10 Specific cooling power as a function of temperature ratio for an expansion ratio, r=1.4.

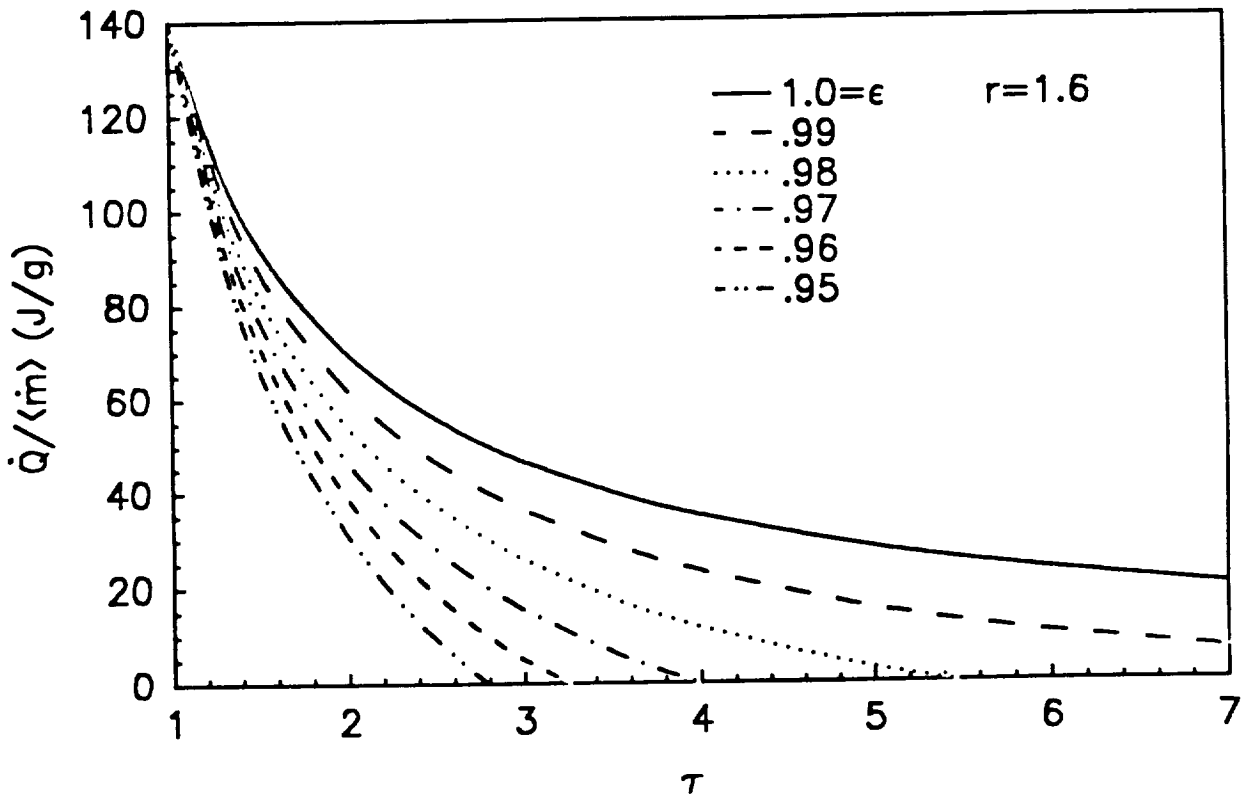

Figure 2.2.1-11 Specific cooling power as a function of temperature ratio for an expansion ratio, r=1.6.

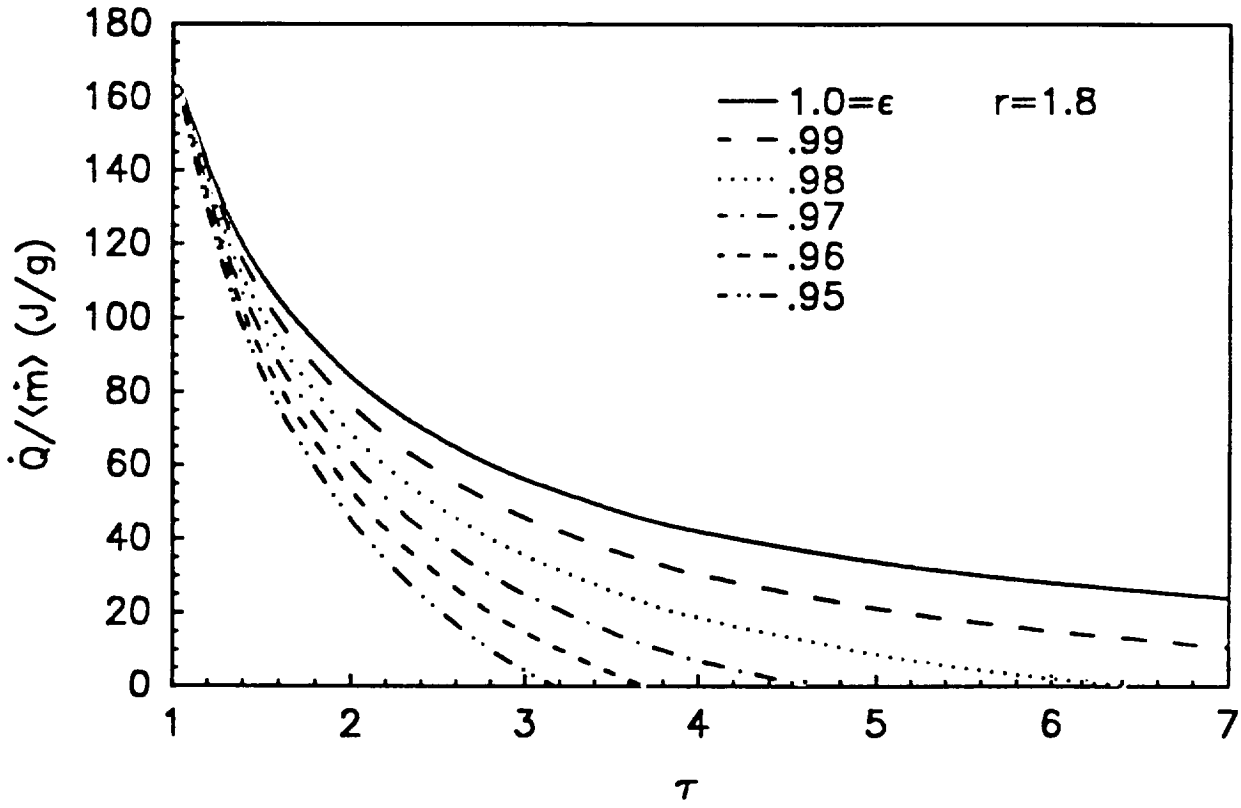

Figure 2.2.1-12 Specific cooling power as a function of temperature ratio for an expansion ratio, r=1.8.

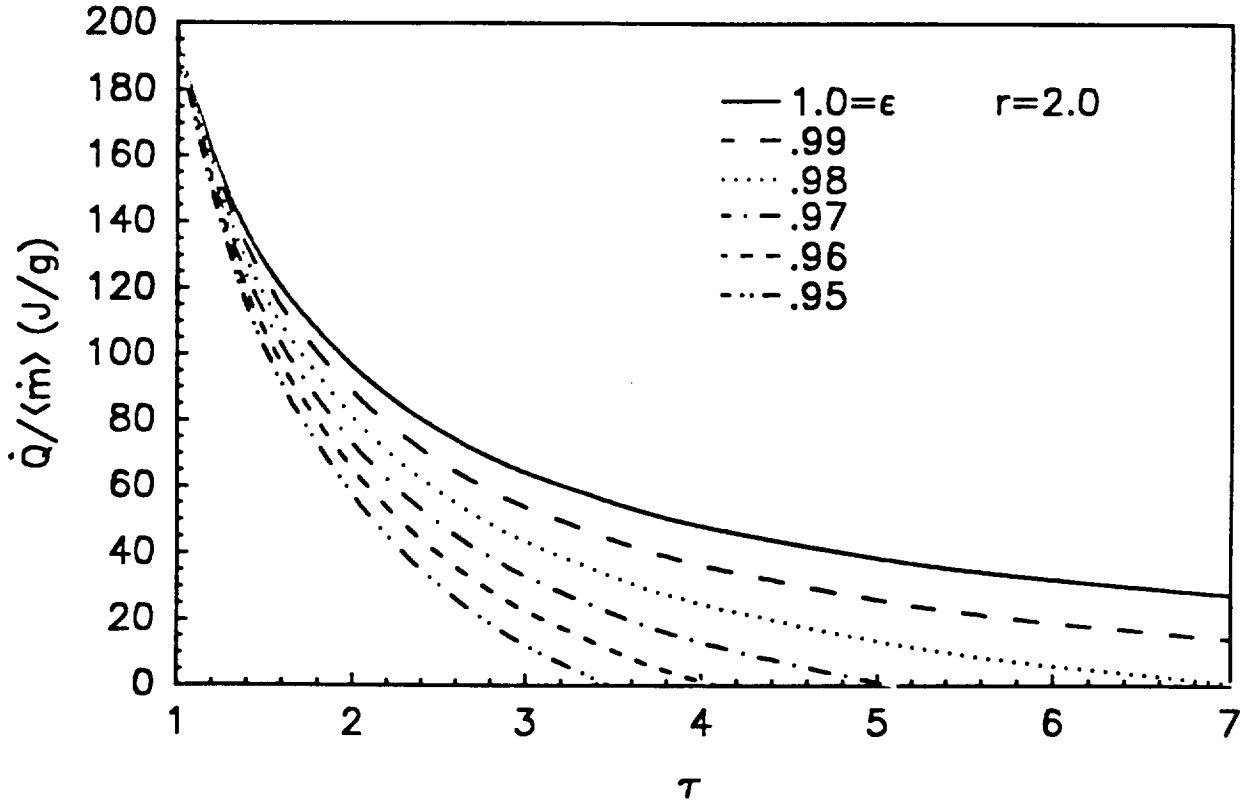

Figure 2.2.1-13 Specific cooling power as a function of temperature ratio for an expansion ratio, r=2.0.

heat of the cold section of the cryocooler, we can determine the effective mass flow into the pulse-tube by measuring the initial cooldown rate of the system. If we have an independent way of measuring the mass flow, this can be used as a check of the process.

b.) If we operate the cryocooler with no heat load (the parasitics must be accounted for) and measure the minimum temperature reached, we can determine the regenerator effectiveness if the volume expansion ratio, r, is known.

c.) If a cryocooler is operated at a fixed expansion ratio, r, but with variable heat input the cryocooler temperature will raise with heat input. The locus of points will lie along a constant effectiveness, ϵ, line.

2.3 Regenerator Model

This section contains a theoretical development of the design of perforated plate regenerators.

The regenerator design equations must provide a link between the design requirements and materials and fluid properties and the regenerator design parameters over which we have control.

The design parameters are:

a. the diameter of the holes in the perforated plates,

b. the diameter of the plates themselves,

c. the number of holes in each plate,

d. the total length of the regenerator.

The design requirements include:

a. the working mass flow,

b. the allowable pressure drop,

c. the properties of the working fluid,

d. the required efficiency.

Regenerator inefficiency may be attributed to two separate effects. The first is the finite temperature difference required to drive the wall-fluid heat transfer, while the second is the finite periodic temperature swing in the matrix caused by the fact that the matrix does not have infinite thermal mass. These inefficiencies contribute to the difference between the actual exit stream temperature and the optimal exit stream temperature (T_L). At the end of the compression (hot blow) stroke, the matrix will have been heated above the lower temperature extreme (T_L). On top of this temperature difference, there will be the wall-fluid temperature difference required to drive the wall-fluid heat exchange. The net temperature difference represents excess heat that is carried into the cold end of the pulse tube, reducing the total cooling power.

In a periodic flow counterflow regenerator with zero dead volume and a high number of NTUs, the temperature distribution along the length of the regenerator can be quite non-linear, as shown in Figure 2.3-1. However, in the regenerators used with a pulse tube, the dead volume can be a significant fraction of the volume of the pulse tube and we may visualize at least part of

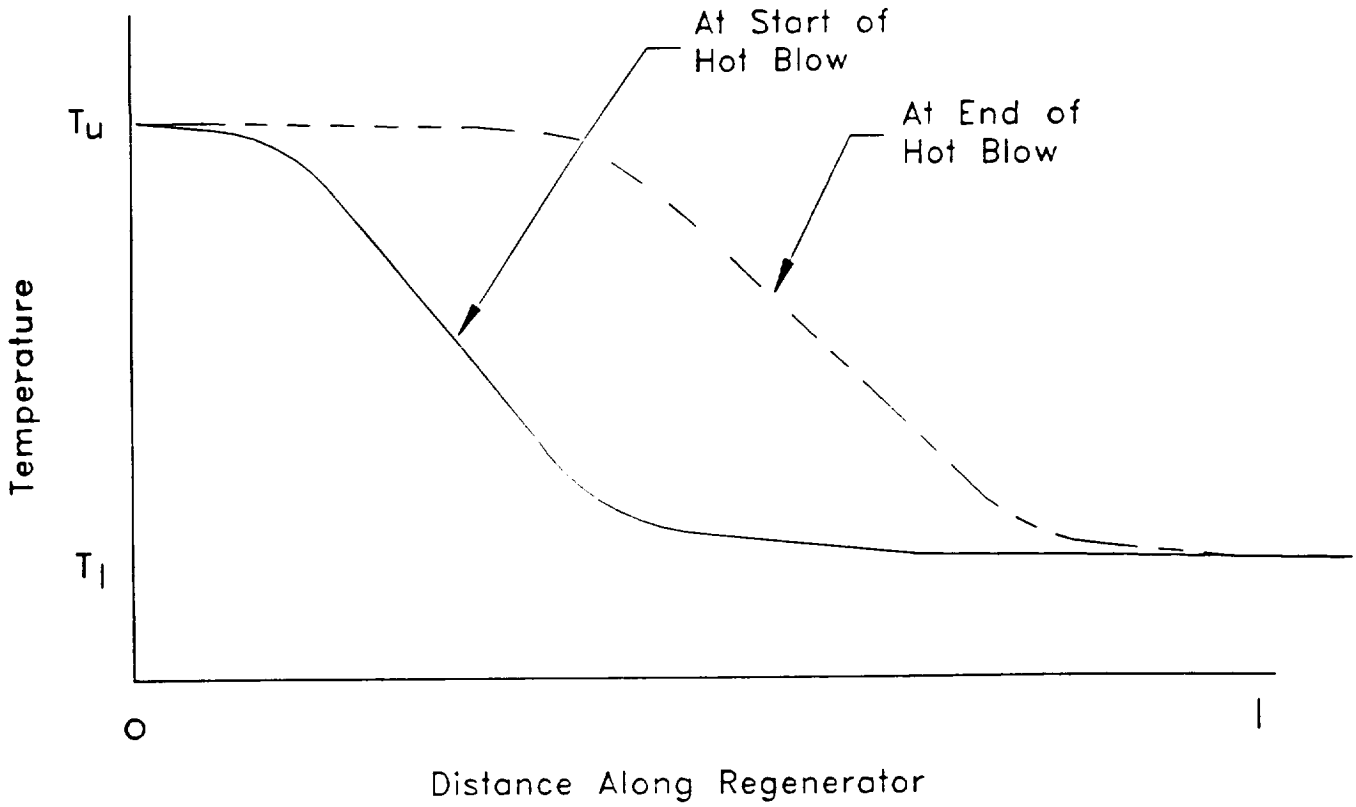

Figure 2.3-1 Temperature distribution along zero dead volume regenerator

the gas as a "plug" that moves into and out of the regenerator, rather than strictly through it. This effect will tend to flatten and linearize the temperature distribution.

We have used the linear temperature distribution shown in Figure 2.3-2. This distribution has the advantage of mathematical simplicity, and is easily seen to be a conservative approximation. It is also quite likely to be a fairly accurate description of the regenerators with finite dead volume. This linear approximation entails (roughly) the following set of implicit assumptions:

a. the capacity of the matrix does not vary along the regenerator,
b. the wall-fluid resistance does not vary along the regenerator,
c. the heat transfer is uniform along the regenerator,
d. the specific heat of the gas is uniform along the regenerator.

All of the variables and symbols used in the following discussion are defined in Figure 2.3-3.

The quantity of interest is the excess heat carried into the cold end of the pulse tube, and can be written in the form:

$$\Delta q = c_p \int_{\text{blowstroke}} (T(t) - T_L)\, \dot{m}(t)dt \qquad (2.3\text{-}1)$$

The temperature of the gas emerging from the lower end of the regenerator is a periodic function.

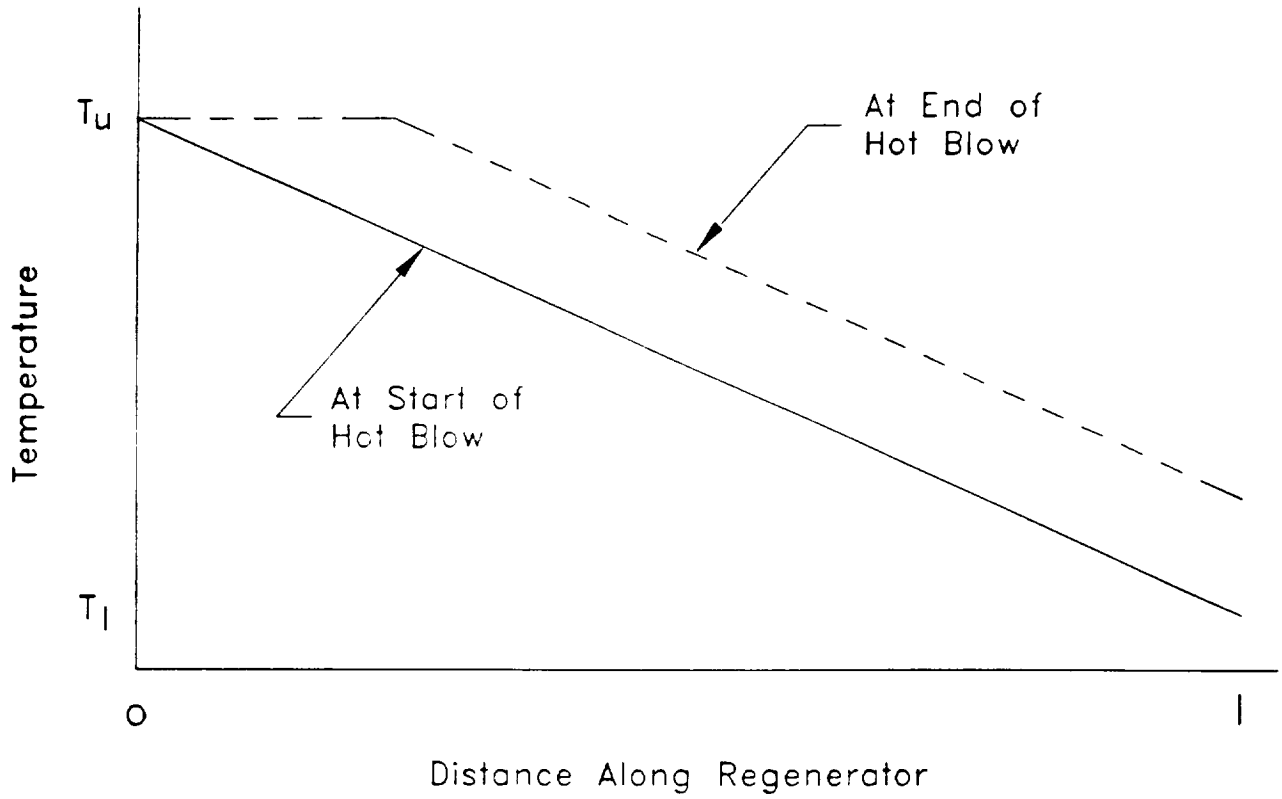

Figure 2.3-2 Linearized temperature distribution along finite dead volume regenerator

T_L	=	Minimum temperature of lower end of regenerator
T_u	=	Temperature at upper end of regenerator
$T(t)$	=	Temperature at lower end of regenerator as a function of time
Δq	=	Excess heat emerging from lower end of regenerator
c_p	=	Specific heat at constant pressure
$\dot{m}_{max}$	=	Maximum mass flow
$\dot{m}(t)$	=	Mass flow as a function of time (roughly sinusoidal)
$<\dot{m}>$	=	Average mass flow
$\Delta T(t)$	=	$T(t) - T_L$
ΔT_{max}	=	Maximum value of $\Delta T(t)$
ΔT_{wf}	=	Maximum value of the wall-fluid temperature difference at the lowerend of the regenerator
ΔT_m	=	Maximum value of the matrix temperature difference at the lower end of the regenerator
ΔT_e	=	Average effective total temperature difference at the lower end of regenerator
h_w	=	Surface heat transfer coefficient
A_w	=	Wall area of the regenerator
τ	=	Period of sinusoidal pressure variation
V_m	=	Volume of the regenerator matrix
C_m	=	Volumetric heat capacity of matrix
$(1-\epsilon)_e$	=	Average effective ineffectiveness of regenerator
$(1-\epsilon)_{wf}$	=	Ineffectiveness due to wall-fluid interaction
$(1-\epsilon)_m$	=	Ineffectiveness due to finite matrix capacity
δ	=	Ratio of $(1-\epsilon)m$ to $(1-\epsilon)wf$
μ	=	Fluid viscosity
L	=	Length of regenerator
ρ	=	Fluid density
D_h	=	Diameter of holes in regenerator plate
N_h	=	Number of holes in regenerator plate
D_p	=	Diameter of regenerator plate
$<\Delta P>$	=	Time-average pressure deop across regenerator
ΔP_{max}	=	Maximum pressure drop across regenerator
Nu	=	Nusselt number
k	=	Fluid thermal conductivity
α	=	Porosity of regenerator plate
DV	=	Dead volume of regenerator

Figure 2.3-3 Definitions of Variables and Symbols Used in Generator Analysis

We have used the (again conservative) assumption that the gas temperature at the lower end of the regenerator is equal to T_L only at the end of the cold blow (expansion) stroke, as shown in Figure 2.3-4. We may write the mass flow at the cold end of the regenerator as:

$$\dot{m}(t) = \dot{m}_{max} \sin(wt) \tag{2.3-2}$$

Noting that the wall-fluid temperature difference is in phase with the mass flow while the matrix term lags by 90 degrees, we can write the temperature at the cold end of the regenerator as:

$$\begin{aligned} T(t) &= (T_L + \Delta T_{max}) + \Delta T_{max} \sin(wt + \delta) \\ &= T_L + (\Delta T_{wf} + \Delta T_m) \\ &\quad + \Delta T_{wf} \sin(wt) + \Delta T_m(-\cos(wt)) \end{aligned} \tag{2.3-3}$$

where ΔT_{wf} and ΔT_m are given by:

$$\Delta T_{wf} = \frac{\dot{m}_{max}\, c_p\, (T_u - T_L)}{h_w A_w} \tag{2.3-4}$$

$$\Delta T_m = \frac{(\tau/4)\, \langle\dot{m}\rangle\, c_p\, (T_u - T_L)}{V_m C_m} \tag{2.3-5}$$

where $\langle\dot{m}\rangle$ is the time-average mass flow.

The heat transferred into the cold end of the pulse tube is then given by:

$$\Delta q = c_p \int_{\text{blowstroke}} \Delta T(t)\, \dot{m}(t)dt \qquad = c_p \int_{\text{blowstroke}} (T(t) - T_L)\, \dot{m}(t)dt \tag{2.3-6}$$

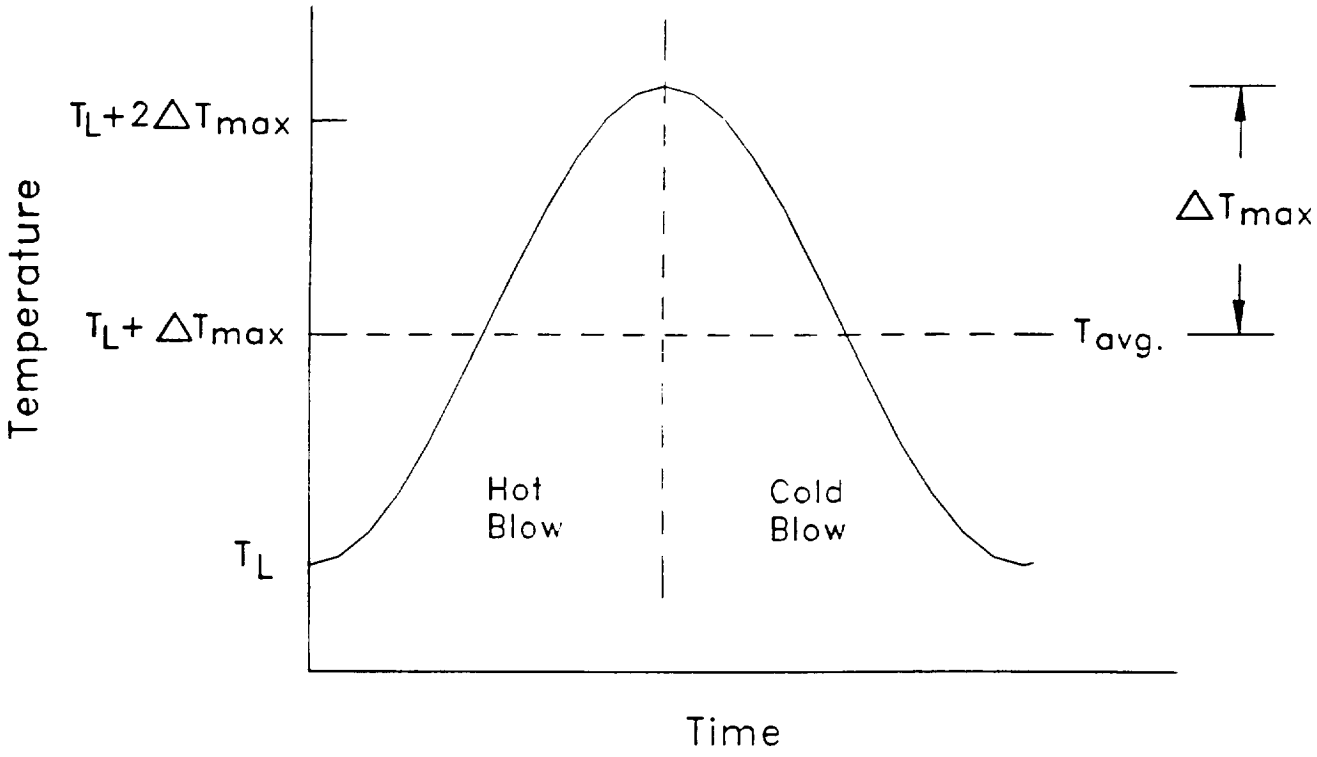

Figure 2.3-4 Gas temperature at cold end of regenerator

$$\Delta q = c_p \left[\int_{\text{blowstroke}} \Delta T_{wf} \, (1 + \sin(wt)) \, \dot{m}_{max} \sin(wt) \, dt + \int_{\text{blowstroke}} \Delta T_m \, (1-\cos(wt)) \, \dot{m}_{max} \sin(wt) \, dt \right] \tag{2.3-7}$$

Examining equation (2.3-7), we are encouraged to define an average effective temperature difference in the form:

$$\Delta T_e = [\Delta T^2_{wf} + \Delta T^2_m]^{1/2} \tag{2.3-8}$$

The efficiency can then be expressed by:

$$(1-\epsilon)_e = 2\Delta T_e/(T_u - T_L) \tag{2.3-9}$$

where the origin of the factor of two in the numerator is clear from Figure 2.3-4. The inefficiency can be written explicitly in terms of the two contributing terms as:

$$(1-\epsilon)_e = [(1-\epsilon)^2_{wf} + (1-\epsilon)^2_m]^{1/2} \tag{2.3-10}$$

The inefficiencies due to wall-fluid term and matrix term can be further parameterized by their ratio, which gives:

$$\delta \equiv (1-\epsilon)_m/(1-\epsilon)_{wf} \tag{2.3-11}$$

$$(1-\epsilon)_{wf} = \frac{(1-\epsilon)_e}{[1+\delta^2]^{1/2}} \tag{2.3-12}$$

and

$$(1-\epsilon)_m = \frac{\delta(1-\epsilon)_e}{[1+\delta^2]^{1/2}} \tag{2.3-13}$$

We are now prepared to develop the design equations for the regenerator. In all cases, the average mass flow <m> is used. The average mass flow is given by:

$$\langle \dot{m} \rangle = \frac{\int_{\text{blowstroke}} \dot{m}(t)dt}{\Delta t_{\text{blowstroke}}} \qquad (2.3\text{-}14)$$

and is related to the peak mass flow through:

$$\langle \dot{m} \rangle = \frac{2}{\pi} \dot{m}_{max} \qquad (2.3\text{-}15)$$

This peak mass flow occurs twice per cycle, once during the compression stroke, and once during the expansion stroke. Since the entrance and return lines for the pulse tube are the same line, the average mass flow for refrigeration purposes is half the average mass flow during the compression stroke.

The average pressure drop is given by:

$$\langle \Delta P \rangle = \frac{128\ \mu \langle \dot{m} \rangle\ L}{\pi \rho\ D^4_h\ N_h} \qquad (2.3\text{-}16)$$

and is related to the peak pressure drop by:

$$\langle \Delta P \rangle = \frac{2}{\pi} \Delta P_{max} \qquad (2.3\text{-}17)$$

As indicated in equation (4), ΔT_{wf} is given by:

$$\Delta T_{wf} = \frac{\dot{m}_{max}\, c_p\, (T_u - T_L)}{h_w A_w}$$

$$= \frac{\pi <\dot{m}> c_p (T_u - T_L)}{2 h_w A_w} \qquad (2.3\text{-}18)$$

where (h_w) is defined in terms of the Nusselt number, fluid, and geometry:

$$h_w = Nu\ k/D_h \qquad (2.3\text{-}19)$$

and ΔT_m is given by:

$$\Delta T_m = \frac{(\tau/4)\ <\dot{m}>\ c_p\ (T_u - T_L)}{V_m C_m} \qquad (2.3\text{-}20)$$

The porosity (α) is defined by:

$$\alpha = \frac{N_h D^2_h}{D_p{}^2} \qquad (2.3\text{-}21)$$

and the total heat exchange area is given by:

$$A_w = \pi D_h N_h L \qquad (2.3\text{-}22)$$

and the matrix volume is given by:

$$V_m = \frac{(1-\alpha)\ \pi\ D^2_p\ L}{4} \qquad (2.3\text{-}23)$$

Inserting (2.3-19), (2.3-22), and (2.3-9) into (2.3-18), we can eliminate (h_w), (A_w), and ($T_u - T_L$) in favor of Nu (the Nusselt number, the actual wall area, and the "wall ineffectiveness" ($(1-\epsilon)_{wf}$) respectively, giving :

$$<\dot{m}>\ c_p = Nu\ k\ N_h\ L\ (1-\epsilon)_{wf} \qquad (2.3\text{-}24)$$

Similarly, substituting (2.3-23) and (2.3-12) into (2.3-20) we can eliminate V_m and $(T_u - T_L)$ in favor of the actual matrix volume and the "matrix effectiveness" $((1-\epsilon)_m)$, giving:

$$2\tau\langle\dot{m}\rangle c_p = \pi(1-\alpha)\, D^2_p\, L\, C_m\, (1-\epsilon)_m \tag{2.3-25}$$

Using (2.3-12) and (2.3-13) to express (2.3-24) and (2.3-25) in terms of the overall effectiveness $(1\text{-epsilon})_e$, we have:

$$[1 + \delta^2]^{1/2} \langle\dot{m}\rangle\, c_p = Nu\, k\, N_h\, L\, (1-\epsilon)_e \tag{2.3-26}$$

and:

$$\frac{[1 + \delta^2]^{1/2}}{\delta}\, 2\, \tau\, \langle\dot{m}\rangle\, c_p = \pi(1-\alpha) D^2_p\, L\, C_m\, (1-\epsilon)_e \tag{2.3-27}$$

Now, rewriting (2.3-16), (2.3-21), (2.3-26), and (2.3-27) to put all the design parameters on the left and all the materials properties and design requirements on the right, we have:

$$D^4_h\, N_h/L = \frac{128\, \mu\, \langle\dot{m}\rangle}{\pi\rho\, \langle\Delta P\rangle} \tag{2.3-28}$$

$$N_h L = \frac{[1 + \delta^2]^{1/2} \langle\dot{m}\rangle\, c_p}{Nu\, k\, (1-\epsilon)_e} \tag{2.3-29}$$

$$D^2_p\, L = \frac{2[1 + \delta^2]^{1/2}\, \tau\, \langle\dot{m}\rangle\, c_p}{\pi\delta(1-\alpha)C_m(1-\epsilon)_e} \tag{2.3-30}$$

$$\frac{D^2_p}{N_h D^2_h} = (1/\alpha) \tag{2.3-31}$$

Identifying the right hand sides of each equation as a design constant, we have:

$$A \equiv \frac{128\ \mu\ \langle\dot{m}\rangle}{\pi\rho\ \langle\Delta P\rangle} \tag{2.3-32}$$

$$B \equiv \frac{[1+\delta^2]^{1/2}\ \langle\dot{m}\rangle\ c_p}{Nu\ k\ (1-\epsilon)_e} \tag{2.3-33}$$

$$C \equiv \frac{2[1+\delta^2]^{1/2}\tau\langle\dot{m}\rangle c_p}{\pi\delta(1-\alpha)\ C_m\ (1-\epsilon)_e} \tag{2.3-34}$$

Solution of this set of equations for D_h, N_h, L, D_p, and the dead volume (DV) yields:

$$D_h = [\alpha C/B]^{1/2} \tag{2.3-35}$$

$$N_h = \frac{[AB^3]^{1/2}}{\alpha c} \tag{2.3-36}$$

$$L = \frac{\alpha c}{[AB]^{1/2}} \tag{2.3-37}$$

$$D_p = \frac{[AB]^{1/4}}{\alpha^{1/2}} \tag{2.3-38}$$

$$DV = \pi\alpha c/4 \tag{2.3-39}$$

Finally, re-expanding the constants into materials properties and design requirements gives:

$$D_h = \left[\ \frac{2\ \alpha\ \tau\ N_u\ k}{\pi\delta(1-\alpha)C_m}\ \right]^{1/2} \tag{2.3-40}$$

$$N_h = 4\delta \left(\frac{1-\alpha}{\alpha}\right)\left(\frac{\langle\dot{m}\rangle C_m}{\tau}\right)\left[\frac{2\pi[1+\delta^2]^{1/2}\ \mu\ c_p}{\rho\ \langle\Delta P\rangle\ Nu^3\ k^3\ (1-\epsilon)_e}\right]^{1/2} \qquad (2.3\text{-}41)$$

$$L = \frac{1}{8}\left(\frac{\alpha}{1-\alpha}\right)\left(\frac{\tau}{C_m\delta}\right)\left[\frac{2[1+\delta^2]^{1/2}\ \rho\ \langle\Delta P\rangle\ Nu\ k\ c_p}{\pi\ \mu\ (1-\epsilon)_e}\right]^{1/2} \qquad (2.3\text{-}42)$$

$$D_p = 4\left(\frac{\langle\dot{m}\rangle}{\alpha}\right)^{1/2}\left[\frac{[1+\delta^2]^{1/2}\ \mu\ c_p}{2\pi\rho\ \langle\Delta P\rangle\ Nu\ k\ (1-\epsilon)_e}\right]^{1/4} \qquad (2.3\text{-}43)$$

$$DV = \left(\frac{1}{2}\right)\left(\frac{\alpha}{1-\alpha}\right)\left(\frac{\delta^2+1}{\delta^2}\right)^{1/2}\left[\frac{\tau\ \langle\dot{m}\rangle\ c_p}{C_m\ (1-\epsilon)_e}\right] \qquad (2.3\text{-}44)$$

The above are the design equations for perforated plate regenerators. They express the design parameters in terms of materials properties, known quantities, and design requirements. The single unspecified quantity appearing on the right of the design equations is (δ), the ratio of matrix ineffectiveness to wall-fluid ineffectiveness. This ratio may be thought of as an optimization parameter. For each value of (δ), there will be a single design meeting the design requirements. The range of designs generated by varying (δ) form an optimization space. For example, if the design is required to optimize regenerator weight for a given (fixed) efficiency, varying delta will generate a range of regenerator designs from one with excellent wall-fluid efficiency and low matrix mass (small δ) to one with relatively poorer wall fluid efficiency and large matrix mass (large δ). The minimum weight will be obtained for a given value of delta, representing the (weight) optimum regenerator.

2.4 Experimental Studies and Results

This section describes the experimental studies conducted in this program, and the results of those experiments. The early studies are discussed briefly, but the bulk of this section is devoted to the most recent experimental results leading to the current "best-effort" prototype design (Sec. 3). Attention is also given to the successful use of the new design and analysis tools in the final stages of this program, including pulse tube and regenerator optimization.

2.4.1 The Regenerator Test Facility

The regenerator test facility is shown in figure 2.4.1-1. This facility was designed to provide performance testing and verification for the periodic counterflow regenerators used in a pulse tube refrigerator. The regenerators are tested under realistic flow and temperature conditions. At room temperature, the facility consists of a gas handling system, a pressure wave generator (compressor), and a heat exchanger for the pressure wave generator. Within the cryostat, the facility has an isothermalizer (to insure that input gas remains at 300K), a liquid nitrogen pot and heat exchanger, connections for the regenerator under test, and pressure and temperature sensors for the inlet (hot) and outlet (cold) end of the regenerator.

The pressure sensors located on the inlet and outlet of the regenerator are are Siemens KPY-14 sensors with a linear operating range of 0-1+ MPa. The sensor bridge is excited by a DC voltage, and the output signal is measured by a high impedance digital multimeter (Dynascan model 2831). The DC component

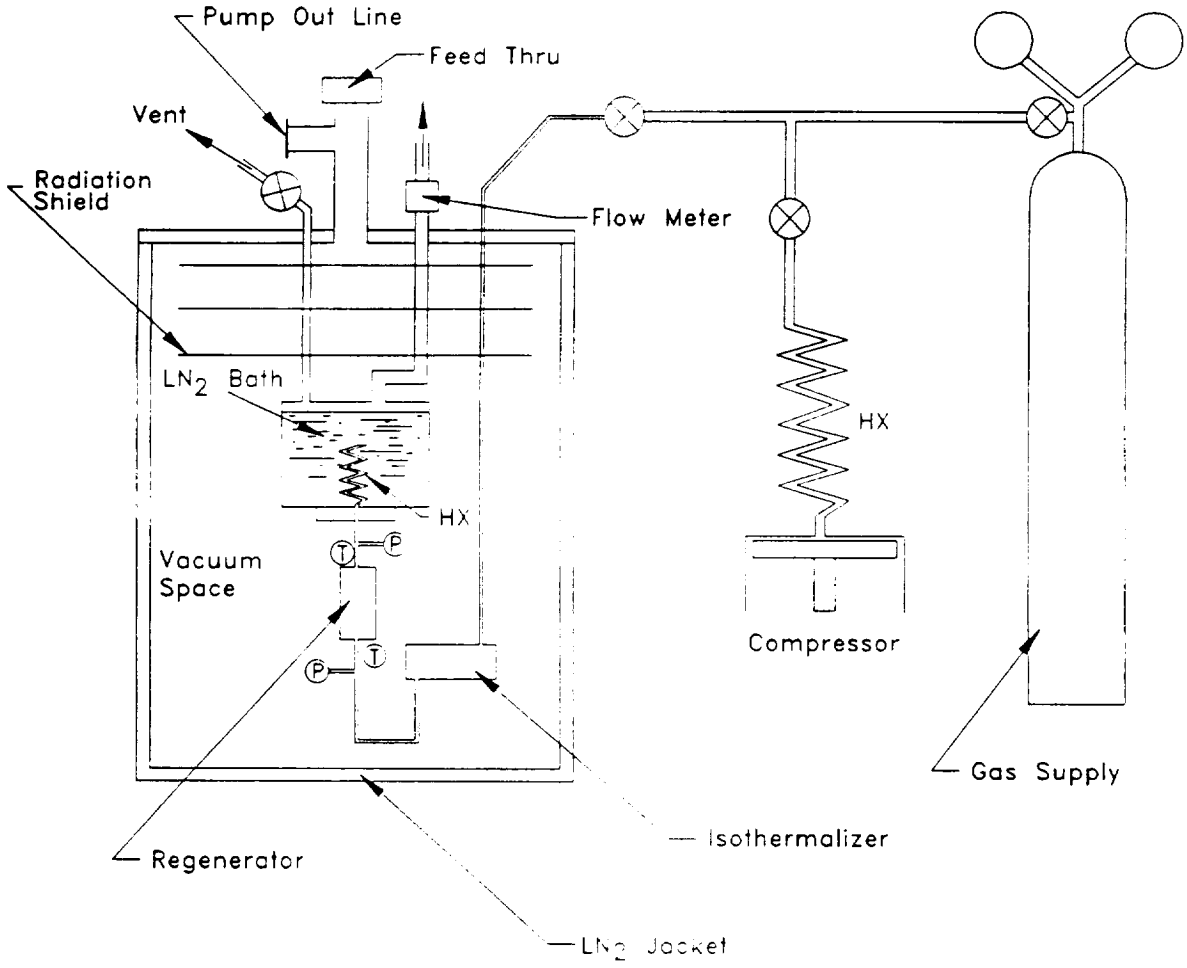

Figure 2.4.1-1 The Regenerator Test Facility

gives the average absolute pressure in the system, and the AC component gives the pressure swing.

Temperature measurement and control are provided by a Lake Shore Cryotronics Model DRC-91C Temperature Controller, and three model DT-470-SD-12 silicon diode sensors. One of these sensors was calibrated by Lake Shore Cryotronics prior to delivery, and we transferred this calibration to the other two sensors. Temperature sensors are located at the inlet and outlet of the regenerator and on the isothermalizer, for which temperature control is provided.

In operation, the system is allowed to come to equilibrium with working pressure in the regenerator, but no periodic pressure swing. This establishes the "baseline" heating delivered to the liquid nitrogen pot. The heating is determined by measuring the boiloff of liquid nitrogen using the flow meter installed in the exit line to the pot. Once the baseline heat load has been determined, the regenerator is driven by a periodic pressure swing generated by the pressure wave generator. Gas moves periodically into and out of the heat exchanger in the liquid nitrogen bath through the regenerator under test. If the regenerator is perfectly efficient, the gas pushed through the regenerator on each compression stroke deposits its heat in the regenerator and is cooled to liquid nitrogen temperature, and reabsorbs this heat as it emerges through the regenerator on the expansion stroke. If the regenerator is not perfectly efficient, there will be a temperature difference between the cold end of the regenerator and the emerging gas, and some heat will be carried into the heat exchanger in the nitrogen pot, resulting in additional boiloff.

Following an initial transient behavior after the pressure wave generator is turned on, the system will again reach equilibrium. The increased boiloff provides a measure of the heat transferred into the heat exchanger as a result of regenerator inefficiency.

The expression for regenerator inefficiency $(1-\epsilon)$ is:

$$(1-\epsilon) = \Delta H \,/\, \dot{m}_{He}\, c_p\, \Delta T \qquad (2.4.1\text{-}1)$$

where:

$$\Delta T = T_{upper} - T_{lower} = 300\ K - 77\ K \qquad (2.4.1\text{-}2)$$

and:

$$\Delta H = (\dot{m}_{LN2} - \dot{m}_{LN2}')\, Q_L \qquad (2.4.1\text{-}3)$$

where $\dot{m}_{LN2}'$ is the mass flow rate of the LN2 boiloff before the pressure wave generator is turned on, $\dot{m}_{LN2}$ is the mass flow rate after the pressure wave generator is turned on, $\dot{m}_{He}$ is the mass flow rate of the helium gas in the regenerator, and Q_L is the latent heat of vaporization.

2.4.2 Pulse Tube Test Facility

The final arrangement for the pulse tube test facility is shown in figure 2.4.2-1. A G.A.S.T. 1HAB-19 compressor was modified to provide a variable volume pressure wave generator, encapsulated in a pressure vessel to remove

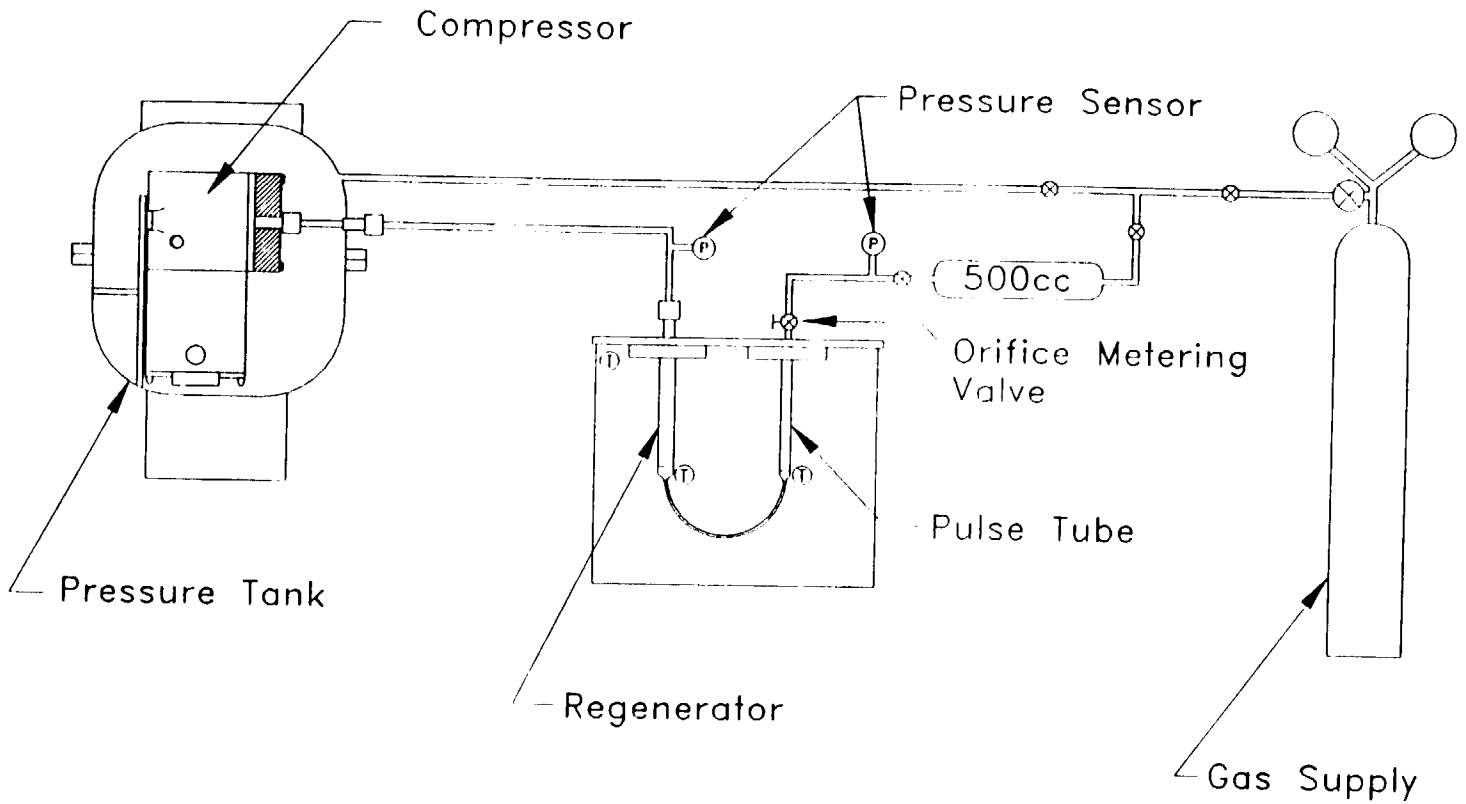

Figure 2.4.2-1 The Pulse Tube Test Facility

the forces associated with the average pressure in the system, and mounted in the immediate vicinity of the top plate of the cryostat. The modifications to the compressor are shown in figure 2.4.2-2 and figure 2.4.2-3.

The compressor is driven by a variable DC power supply, from which the driving voltage and current can be measured, allowing us to compute the total electrical input power to the pulse tube refrigerator.

Pressure sensors are located on the downstream end of the connecting line immediately above the entrance into the cryostat, and on the connecting line between the hot end of the pulse tube and the orifice volume, downstream of the orifice valve.

The pressure sensor located on the connecting line is a Siemens KPY-14. The sensor bridge is excited by a DC voltage, and the output signal is measured by a digital multimeter. The DC component gives the average absolute pressure in the system, and the AC component gives the pressure swing at the downstream end of the connecting line.

The pressure sensor located between the orifice valve and the orifice volume is a SETRA model 205-2. This sensor is calibrated to provide accurate pressure measurements from 0 to 3.4 MPa The DC component again provides the average absolute pressure, and the AC component provides the pressure swing. To measure the pressure ratio in the hot end of the pulse tube, the valve between the pressure sensor and the orifice volume is fully closed, and the orifice valve is opened completely. The pressure swing (AC component) is measured with both a digital multimeter, and an oscilloscope. The RMS value

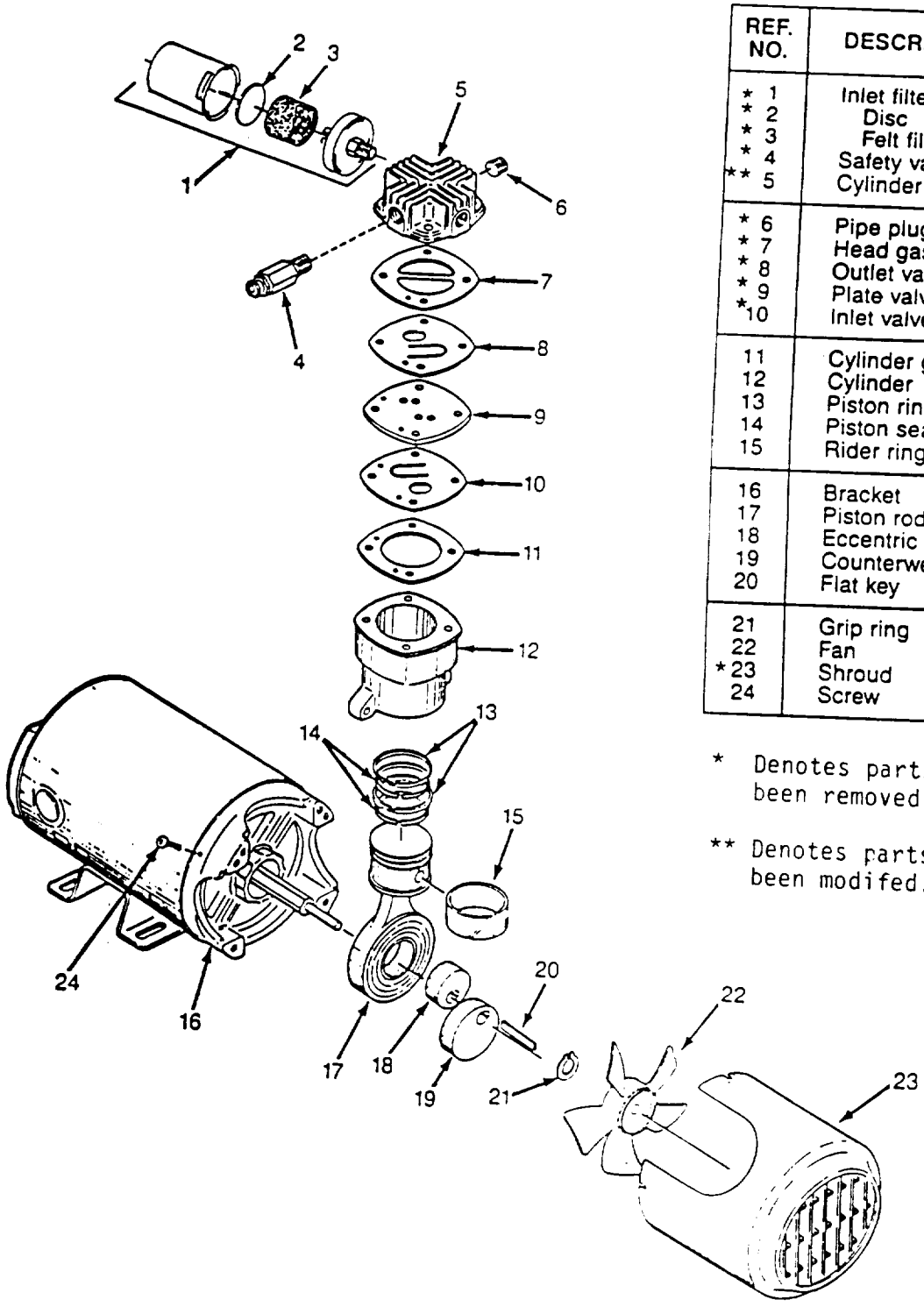

REF. NO.	DESCRIPTION
* 1	Inlet filter assembly
* 2	Disc
* 3	Felt filter
* 4	Safety valve assembly
** 5	Cylinder head
* 6	Pipe plug
* 7	Head gasket
* 8	Outlet valve
* 9	Plate valve
* 10	Inlet valve
11	Cylinder gasket
12	Cylinder
13	Piston ring
14	Piston seal
15	Rider ring
16	Bracket
17	Piston rod assembly
18	Eccentric
19	Counterweight
20	Flat key
21	Grip ring
22	Fan
* 23	Shroud
24	Screw

* Denotes parts which have been removed.

** Denotes parts which have been modifed.

Figure 2.4.2-2 Modifications to the G.A.S.T. model 1HAB-19 compressor

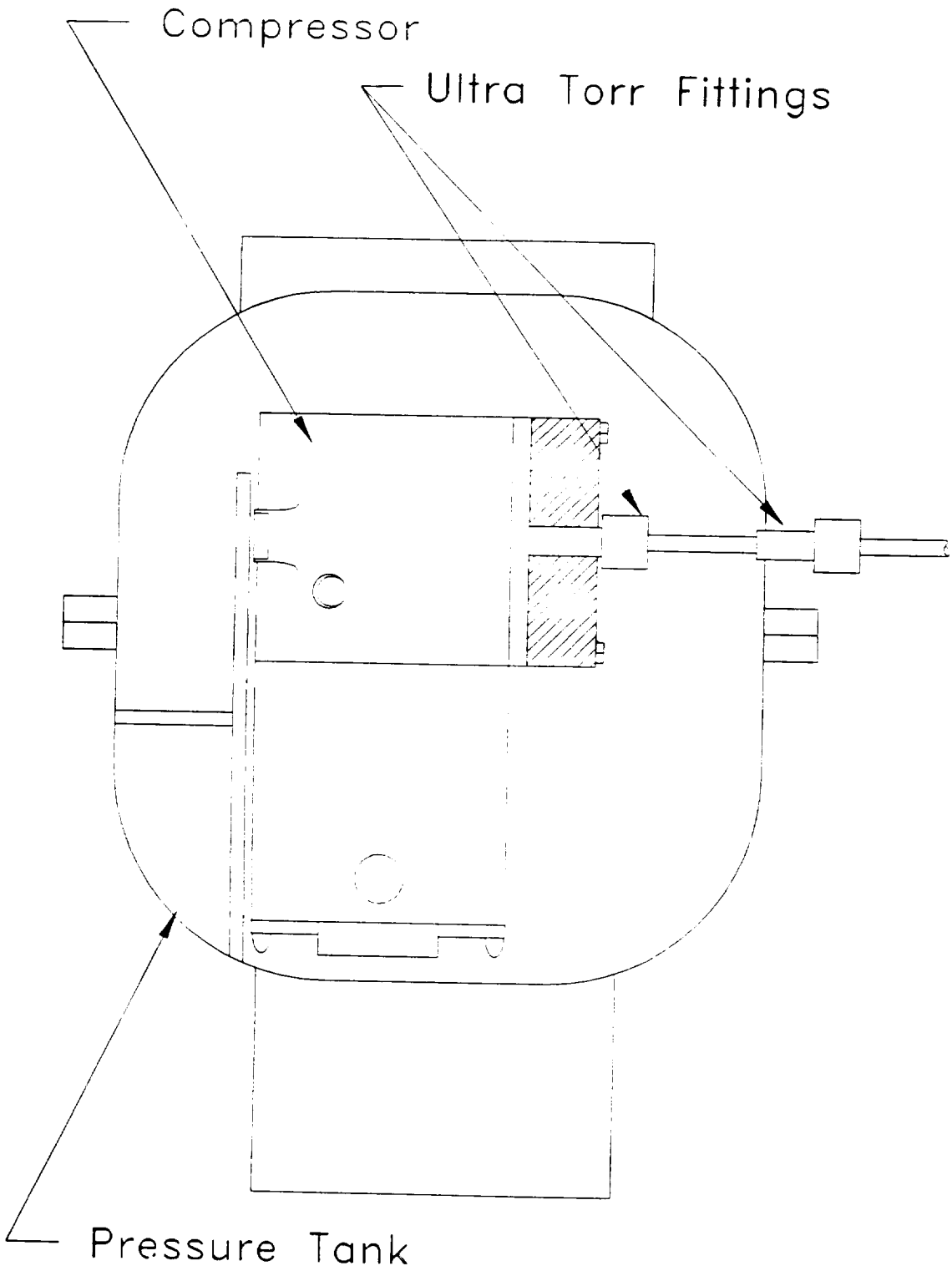

Figure 2.4.2-3 Encapsulation of modified compressor

provided by the DMM agrees well with the measurements made using the oscilloscope, and the waveform is approximately sinusoidal.

In all cases, the pressure ratio is computed by assuming that the pressure swing is symmetrical about the average pressure. The peak swing is added to the average pressure to obtain P_{max}, the peak swing is subtracted from the average pressure to obtain P_{min}, and the pressure ratio is given by:

$$R_p = P_{max} / P_{min} \qquad (2.4.2\text{-}1)$$

In the interest of obtaining a better picture of the distribution of pressure drops and mass flows in the pulse tube system, several attempts were made to install a KPY-14 pressure sensor on the connecting line between the cold end of the regenerator and the cold end of the pulse tube. These attempts were unsuccessful. Because of its sensitivity to heat, the KYP sensor could not be hard soldered into the line, and neither soft solder nor epoxy proved reliable for use at low temperatures with 10 Atm. average pressure and 1.5 Atm. periodic pressure swings.

The SETRA gage also provided a crude means of measuring the mass flow into and out of the hot end of the pulse tube during run. The AC signal from the SETRA gage with the orifice valve in the running position, and the orifice volume connected was near the lower limit of resolution, but could be measured approximately to give an estimate (within ~30%) of the mass flow between the hot end of the pulse tube and the orifice volume.

Temperature measurement and control are provided by a Lake Shore Cryotronics Model DRC-91C Temperature Controller, and three model DT-470-SD-12 silicon diode sensors.

One of the temperature sensors is installed at the top plate of the cryostat to monitor the temperature of the gas delivered by the pressure wave generator, while the other two are installed at the cold ends of the regenerator and pulse tube respectively.

To provide information on the thermal distribution along the regenerator the temperature sensor from the cold end of the pulse tube was moved to the geometric center of the regenerator on at least one occasion,.

A heater is provided at the lower end of the regenerator (consistent with Radebaugh's placement). This heater consists of 28 cm of 40 gauge (3 mil) Manganin wire, with a total resistance of 25 Ohms. The heater is wound in intimate thermal contact with the lower (cold) end of the regenerator, is driven by a Lambda LA-200 power supply, and the input voltage is measured using a digital multimeter. The applied heat load was taken to be:

$$\dot{Q} = V^2 / R \qquad (2.4.2\text{-}2)$$

No attempt was made to use a 4-wire arrangement for the heater, since the copper leads to the heater dissipate a negligible fraction (< 1%) of the applied power.

2.4.3 Early Studies

The regenerator test facility was used to measure the performance of several early regenerator designs, two of those are discussed here. The regenerators were:

a. a perforated plate regenerator 0.30 cm in diameter, 7.5 cm in length, and containing 233 perforated copper plates with 340 34x100 micron holes,

b. a screen regenerator 0.63 cm in diameter, 7.5cm in length containing 1100 discs of 400 mesh stainless steel wire cloth.

The regenerators were tested using the facility and techniques described in section 2.4.1 above. The results were:

a. the perforated plate regenerator had an efficiency of 99.3% with a mass flow of 0.023 g/s, and a measured pressure drop of 0.146 MPa,

b. the screen regenerator had an efficiency of 99.4% with a mass flow of 0.031 g/s, and a measured pressure drop of 0.088 MPa.

These results demonstrated that the perforated plate regenerator had higher efficiency than a screen regenerator with the same envelop. However, the mass flows required for an 80K 0.25W pulse tube refrigerator were projected to be sufficiently high that the required efficiency could not be obtained using the (then) available small diameter (0.27 cm) perforated plate material.

Regenerator design continued with both screen and larger diameter perforated plate material as it became available. In many cases, the use of screens allowed significantly more design freedom, especially since production model regenerators would still be implemented in perforated plate material with one or a mixture of the following advantages:

a. better efficiency and lower dead volume in the same envelop
b. equal efficiency and lower dead volume in a smaller envelop

Because of the sometimes unexpected interactions of the various components of the pulse tube refrigerator, separate regenerator testing was gradually abandoned in favor of system testing on the Pulse Tube Test Facility.

A number of tests of complete pulse tube refrigerators were performed using the Pulse Tube Test Facility and the 290cc pressure wave generator. The best performance was achieved using a regenerator 2.54 cm in diameter, 7.0 cm in length, and containing 700 discs of 400 mesh stainless steel wire cloth, and a pulse tube 1.27 cm in diameter, 24 cm in length with 80 mesh copper screen heat exchangers. This combination reached an ultimate temperature of 102K.

The early tests indicated that the original models of pulse tube and regenerator performance were inadequate to the task of establishing an a-priori design that would meet the program requirements. Much of this early work was devoted to exploring the interaction of the compressor, regenerator, and pulse tube, and developing a qualitative understanding of system performance.

Based on these early experiments and that qualitative understanding, the generalized analysis approach to pulse tube performance (Sec 2.2) gradually evolved, along with a simplified approach to modeling regenerators (Sec 2.3). At the same time, it became clear that the 290cc compressor was not a good match to the volumes of the pulse tube refrigerators of interest in this program, and the decision was made to augment the test facility with a much smaller pressure wave generator.

2.4.4 Studies with the 20cc Pressure Pressure Wave Generator

Once it became clear that a better volume match between the compressor and the pulse tube system was required to make experimental progress, we installed the modified G.A.S.T compressor (discussed in section 2.4.2). Rapid progress was made using this compressor, and a temperature of 116 K was reached using a perforated plate regenerator 0.95 cm in outside diameter, 11 cm in length, containing 120 F-61 perforated plates of graded length (as described below) and a pulse tube 0.95 cm in outside diameter, 12 cm in length, with F-61 perforated plug heat exchangers, as described in figure 2.4.4-3. The F-61 material is 0.89 cm (0.350 inch) diameter with 3781 holes 95 microns in diameter.

Pulse Tube Optimization. At this point, we elected to optimize the pulse tube to the regenerator. To determine the effects of pulse tube volume (and consequently R_p and the mass flow), this regenerator was used with a selection of six different pulse tubes, described in figure 2.4.4-1. As expected, the ultimate temperature reached by these pulse tube / regenerator combinations depended on the pressure ratio R_p and mass flow in the pulse tube. The

Regenerator	OD (in)	OD (cm)	Wall (in)	ID (in)	ID (cm)	len (cm)	Heat Ex
A	0.500	1.270	0.020	0.460	1.168	6.3	25 80 Mesh Cu Screens
B	0.250	0.635	0.010	0.230	0.584	11.0	25 80 Mesh Cu Screens
C	0.375	0.953	0.010	0.355	0.902	14.5	25 80 Mesh Cu Screens
D	0.375	0.953	0.010	0.355	0.902	11.0	1cm F-61 slugs
E	0.375	0.953	0.010	0.355	0.902	8.6	25 80 Mesh Cu Screens
F	0.375	0.953	0.010	0.355	0.902	5.8	25 80 Mesh Cu Screens
G	0.375	0.953	0.010	0.355	0.902	11.0	25 80 Mesh Cu Screens

Figure 2.4.4-1 Physical description of pulse tubes used in optimization

summary results are shown in figure 2.4.4-2. The ultimate temperature is reduced as the pulse tube volume is decreased because the regenerator operates more efficiently with lower mass flow. This trend continues as the mass flow is further reduced, until the remaining mass flow is insufficient to support the heat leaks into the cold end through the regenerator and the walls of the pulse tube.

This study indicated that the 11cm pulse tubes were near the optimum for the perforated plate regenerator, and that whether the heat exchangers were made of F-61 plugs or 80 mesh copper screen had little effect on the ultimate temperature. The ultimate temperature for the plate regenerator and the 12cm pulse tubes was between 116 and 118K, at a pressure ratio of 1.44.

Regenerator Optimization. Using the 0.95 cm diameter by 12 cm pulse tube with screen heat exchangers (PT-G), we embarked on a program of regenerator optimization. To reduce the lead time associated with acquisition of the perforated plates, and to retain design flexibility, we elected to develop a series of screen regenerators, beginning with one that closely approximated the perforated plate design.

The hole size in the F-61 plates is 95 micron, closely matching the edge dimension (~ 103 micron) of the holes in 150-mesh stainless screen. However, based on the graphs in Kays and London (1985), the screens are expected to have a higher friction factor than the perforated plates for the same number of comparable holes and the same overall length. In an effort to maintain or improve the wall-to-fluid thermal contact at the cold end and not introduce an intolerable pressure drop across the regenerator, we selected a graded design

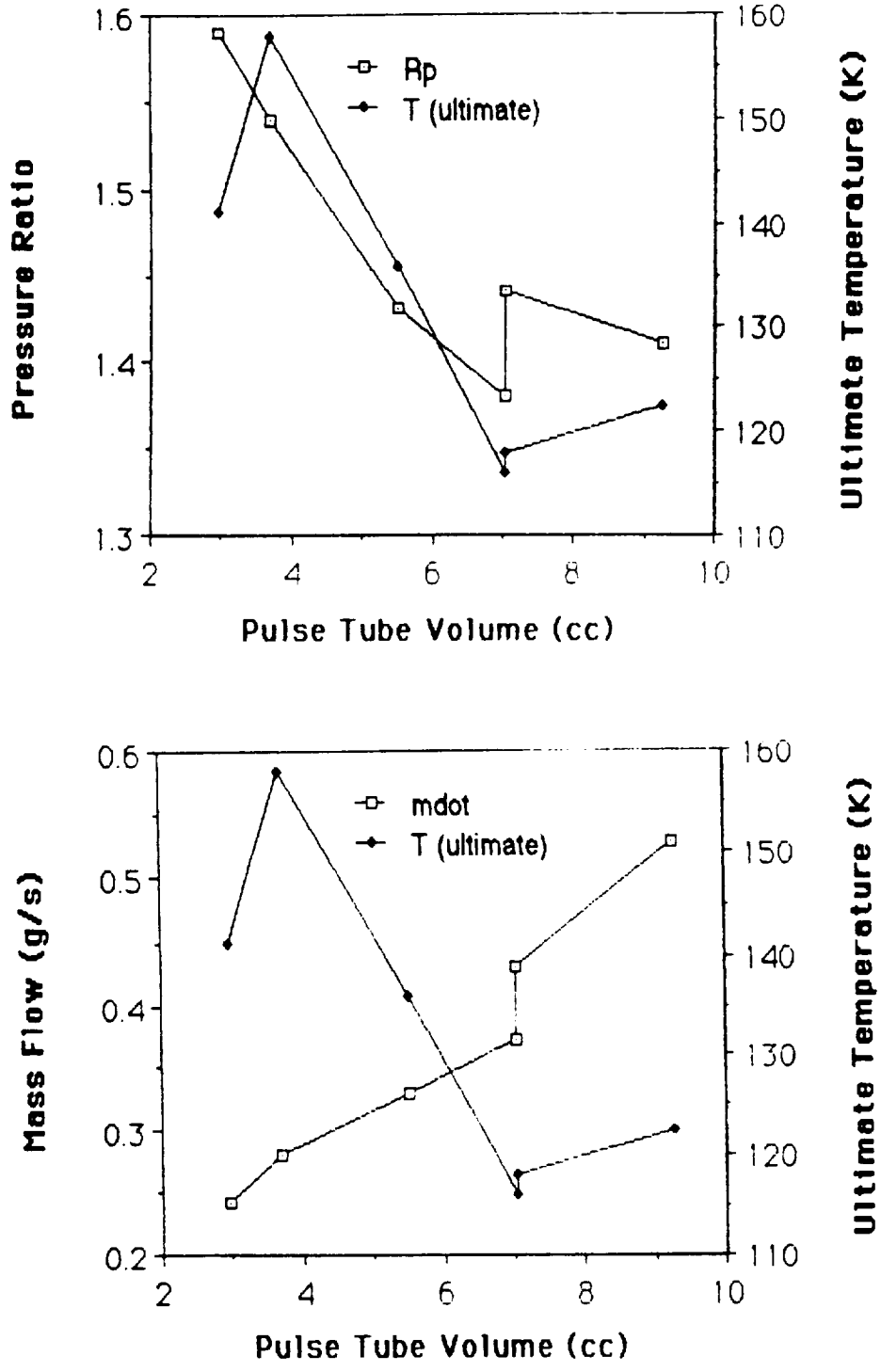

Figure 2.4.4-2 Results of pulse tube optimization. The upper graph shows the pressure ratio and ultimate temperature as a function of pulse tube volume, while the lower graph shows mass flow and ultimate temperature as a function of pulse tube volume.

(regenerator O in figure 2.4.4-3) with a diameter of 1.27 cm, and a total active length of 12cm containing approximately equal lengths (4cm each) of 100-mesh (160 discs), 150-mesh (200 discs), and 200-mesh (250 discs). This regenerator was operated with PT-G the reached a temperature of 87.1K, at a pressure ratio of 1.28, indicating much improved regenerator efficiency, and somewhat lower mass flow.

Encouraged by the agreement between predicted and measured performance of this pulse tube / regenerator combination, we elected to build a second graded regenerator (R-J) with a diameter of 1.91cm (3/4 inch), a length of 6cm, again equally divided between 100-, 150-, and 200-mesh stainless steel screens. This regenerator was expected to provide performance comparable to R-O with lower pressure drop. The performance was significantly worse, with an ultimate temperature of 128.6K at a pressure ratio of 1.28. The degraded performance was attributed to the formation of "jets" at the entrance and exit of the regenerator where 1/4 inch and 1/8 inch OD connecting lines join. It was also noted, however, that the pressure ratio was unchanged, indicating that the pressure drop in R-O was insignificant.

Based on the fact that the pressure drop in R-O was not the limiting factor in the system performance, we designed another graded regenerator (R-X) with a diameter of 1.27 cm, and a total active length of 12cm containing approximately equal lengths (3cm each) of 100-mesh (100 discs), 150-mesh (152 discs), 200-mesh (188 discs) and 250-mesh (246 discs). This design was expected to provide significantly higher efficiency with a corresponding increase in pressure drop across the regenerator (as shown in figure 2.4.4-4).

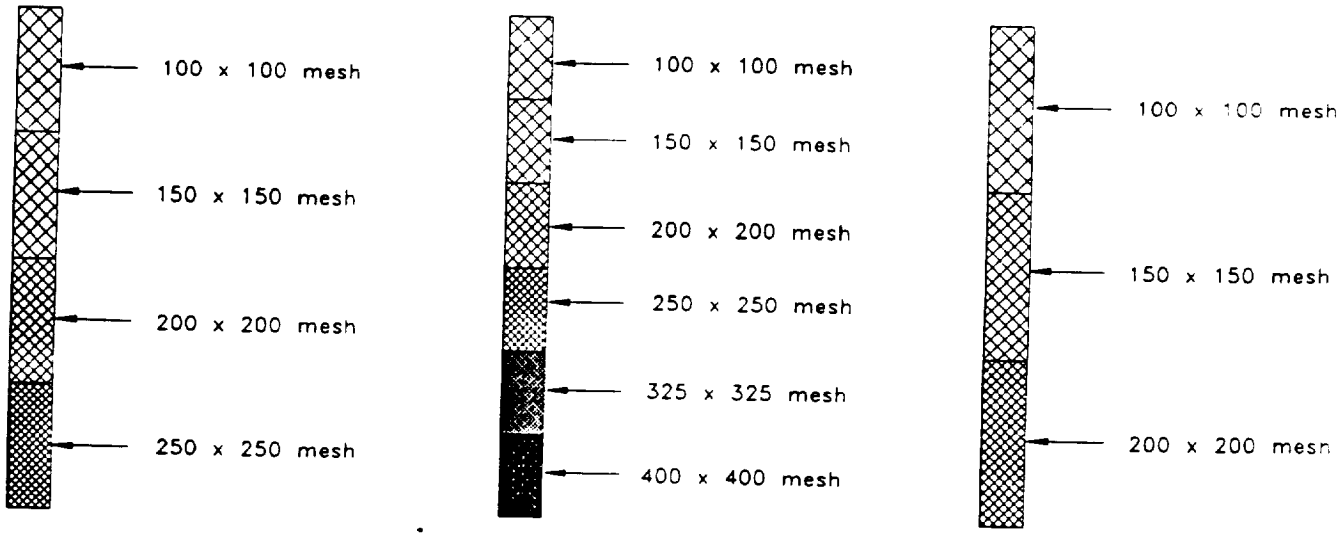

Screen Regenerators
12 cm long

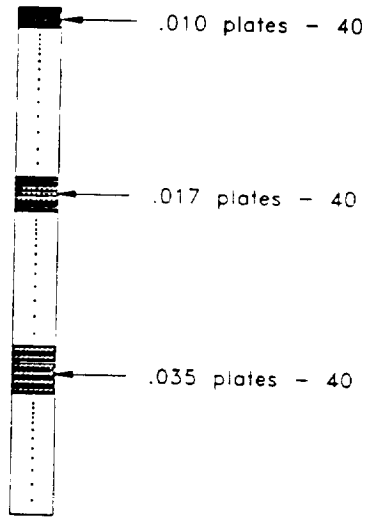

Plate Regenerators
11 cm long

Figure 2.4.4-3 Designs for four graded regenerators. Regenerator-X is at upper left. Regenerator-Y is in upper middle. Regenerator-O is at upper right, and regenerator-H is in lower middle.

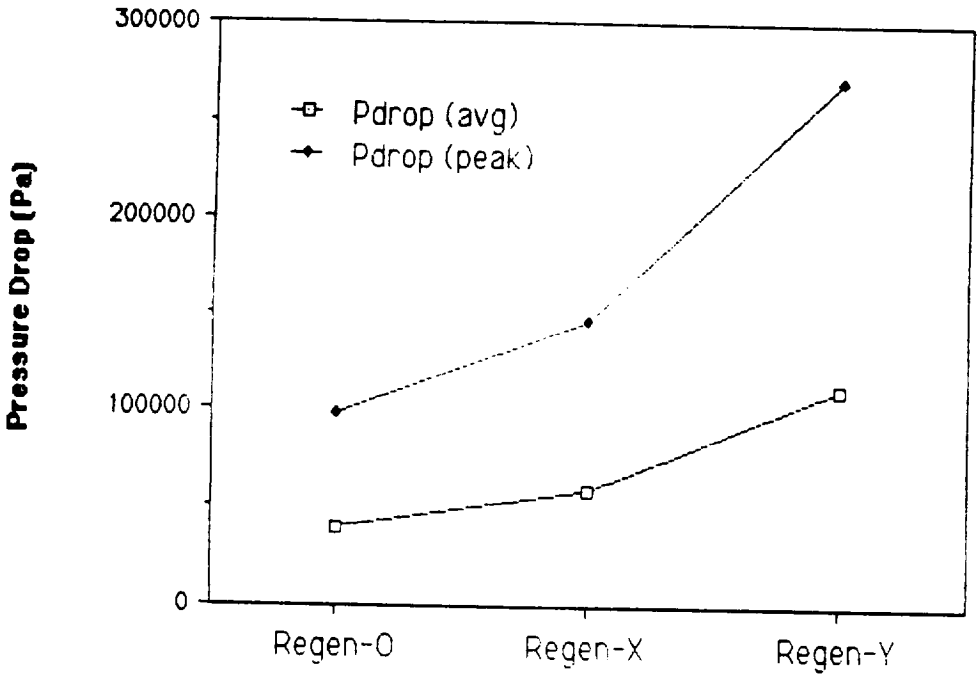

Figure 2.4.4-4 Predicted pressure drops for regenerators O, X, and Y.

This design was tested with PT-G and the ultimate temperature reached was 77.9K with liquid nitrogen in the jacket of the cryostat (to reduce radiative load) and a gas supply temperature of 300K, maintained by cold nitrogen flow in the heat exchanger on the connecting line. Without liquid nitrogen in the cryostat jacket and using water in the heat exchanger on the connecting line, the inlet temperature was 304K, and the ultimate temperature was 82.8K, at a pressure ratio of 1.28.

Noting again that the pressure ratio had not declined, indicating that the total pressure drop across the regenerator was not yet the limiting factor in system performance, we designed a final graded regenerator (R-Y) with six graded screen sections. R-Y has a diameter of 1.27 cm, and a total active length of 12cm containing approximately equal lengths (2cm each) of 100-mesh (60 discs), 150-mesh (104 discs), 200-mesh (128 discs), 250-mesh (164 discs), 325-mesh (188 discs) and 400-mesh (240 discs). The predicted pressure drop for this regenerator is approximately twice that for R-X, as shown in figure 2.4.4-4.

This regenerator was tested with PT-G, and an ultimate temperature of 77K was reached with water in the heat exchanger on the connecting line and no liquid nitrogen in the cryostat jacket. The pressure ratio was between 1.22 and 1.25, indicating that the pressure drop in the regenerator was becoming significant in the computation of pressure and mass flow distributions.

This pulse tube / regenerator combination is the current baseline, and its physical characteristics and performance are described in detail below.

3.0 CURRENT PROTOTYPE

This section describes the current prototype in detail, along with analytical predictions and measured performance. Bear in mind, that although the current prototype almost meets the requirements of a 0.25 Watt 80K cryocooler, it is not considered a finished item. Specifically, it would benefit dramatically from a reimplementation of its regenerator in perforated plates, with a corresponding decrease in regenerator dead volume, or a corresponding increase in wall-to-fluid conduction.

3.1 Physical Description

The current prototype consists of the following:

a. A variable frequency pressure wave generator
   Effective displacement of approximately 17.5 cc. (sec. 2.1)
   Frequency 12-30 Hz approx.

b. Upper Connecting Line (compressor -> regenerator)

OD:	1/4 inch (0.635 cm)
ID:	0.186 inch (0.472 cm)
Length:	14.75 inch (37.5cm)
Volume:	6.57 cc

   6 inch concentric tube counterflow gas -> water heat exchanger

c. Regenerator

OD:	1/2 inch (1.27 cm)
ID:	0.480 inch (1.22 cm)
Length:	12 cm active length, 2x 1.25cm end caps
Dead Volume:	11.35 cc
Flow Control:	25 80-mesh copper cloth discs in each end cap
Screens:	60 100-mesh
	104 150-mesh
	128 200-mesh
	164 250-mesh
	188 325-mesh
	240 400-mesh

d. Lower Connecting Line

OD:	1/8 inch (0.318 cm)
ID:	0.061 inch (0.155 cm)
Length:	10 cm
Volume:	0.19 cc

e. Pulse Tube

OD:	3/8 inch (0.95 cm)
ID:	0.355 inch (0.90 cm)
Length:	11 cm active length, 2x 1.25cm end caps
Volume:	8.2 cc
Heat Ex:	25 80-mesh copper cloth discs on each end

f. Orifice Volume: 500cc

The operating conditions for which the the current prototype reached 77K were:

Frequency	25 Hz
Average Pressure	0.96 MPa
Pressure Ratio	1.47 (at regenerator inlet)
Pressure Ratio	1.25 (at hot end of pulse tube)
Pressure Swing	7-10 KPa (at hot end of pulse tube, operating)
Inlet Temperature	305 K (at top plate)
Ultimate temperature	77 K (cold end of pulse tube)

The pressure swing measured at the entrance to the orifice volume during operation is 7-10 KPa (peak-to-peak). From this the displaced volume of gas being pushed out of the pulse tube can be obtained:

$$V_{displaced} = [\Delta P_{orifice} / P_{average}] * V_{orifice} \qquad (3.1\text{-}1)$$

This results in a displaced volume of 2.7cc - 4.2cc, which is generally consistent with the belief that 1/3 of the effective volume in the pulse tube is pushed into and out of the orifice volume at each stroke. Temperature corrected to 300K, the upper (warmer) 1/3 of the pulse tube volume is 3.4cc

Mass Flow. If the mass flows are calculated as discussed in section 2.1, the mass flow at the exit of the compressor is 1.35 g/s, the mass flow at the entrance to the regenerator is 1.01 g/s, the mass flow at the entrance to the pulse tube is 0.47 g/s, and based on the pressure swing at the entrance to the orifice volume, the mass flow through the orifice is between 0.21 and 0.32 g/s

3.2 Analytical Predictions

Based on these pressures, pressure ratios, and mass flows, it is possible to predict the cooling power of the current prototype as a function of temperature. From generalized analysis, the equation that has been used is:

$$\frac{\dot{Q}_R + \dot{Q}_A}{\dot{m}} = \left(\frac{RT_E}{3m_0}\right)\left(\frac{\gamma}{\gamma-1}\right)\left[1 - (1/(r^{\gamma-1})) - 3(\tau-1)(1-\epsilon)\right] \qquad (3.2\text{-}1)$$

where m_0 is the molar mass, r is the pressure ratio at the entrance to the pulse tube, τ is the temperature ratio (T_{upper} / T_{lower}), ϵ is the regenerator

efficiency, $\dot{m}$ is the mass flow, and $\dot{Q}_R$ is the residual heat load (from radiation and conduction), and $\dot{Q}_a$ is the applied heat load.

Two tests of cooling power vs temperature were run at different pressures, as discussed below. Using the measured pressure ratios and computed mass flows for these runs, the predicted cooling power was computed as a function of temperature as shown in figure 3.2-1.

In this treatment, $(1-\epsilon)$ has been used as a single fit parameter, and is determined from the no-load performance of the system. The residual heat ($\dot{Q}_R$) is, in effect, a second fit parameter, but the computed cooling power is insensitive to $\dot{Q}_R$, as seen in Figure 3.2-1.

3.3 Measured Performance

In preparation for measuring the cooling power of the current baseline, pulse tube PT-G was replaced by PT-D which is physically identical except that the heat exchangers are made of 1 cm slugs of F-61 perforated plate material. This change was made because the thermal contact between the pulse tube heat exchangers and the gas in the pulse tube is calculated to be better by a factor of 3 using the F-61 plugs. This is unimportant with low heat loads, but becomes progressively more important as higher loads are applied. Although the baseline system had been operating at 77K with PT-G, the lowest temperature reached with PT-D was 83.7 K at the cold end of the regenerator and 81 K at the cold end of the pulse tube.

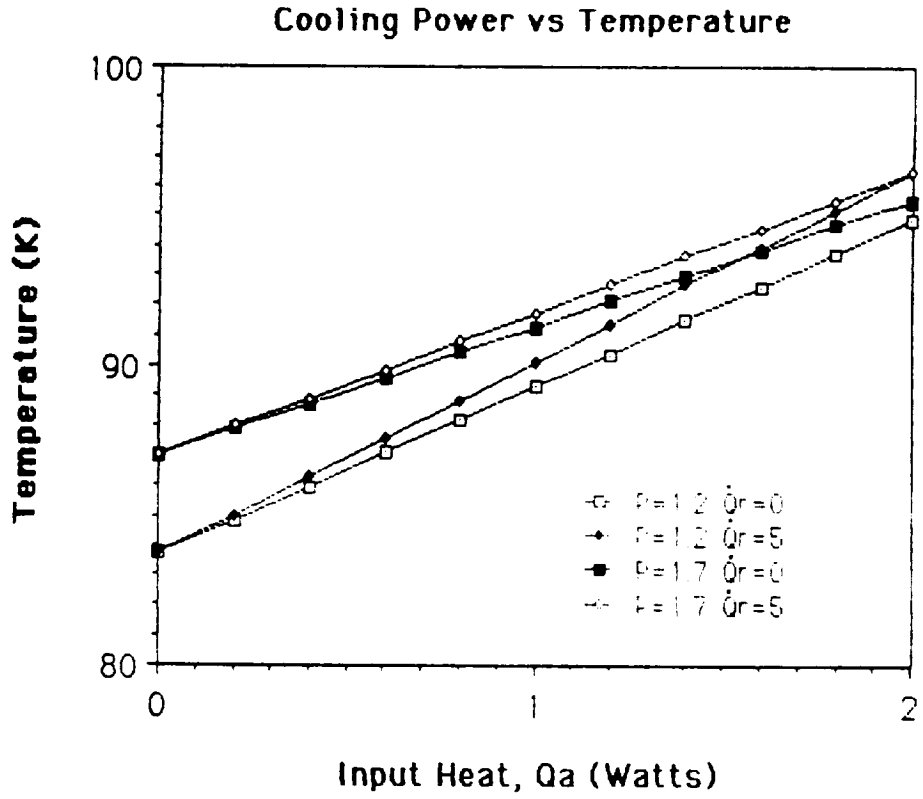

Figure 3.2-1 Predicted cooling power as a function of temperature for the current prototype using PT-D

Two tests of cold end temperature as a function of applied heat load were made, under the following conditions:

Run 1:	Frequency	22 Hz
	Average Pressure	1.19 MPa
	Pressure Ratio	1.47 (at regenerator inlet)
	Pressure Ratio	1.27 (at hot end of pulse tube)
	Pressure Swing	7-10 KPa (hot end of pulse tube, operating)
	Inlet Temperature	305 K (at top plate)
	Ultimate temperature	81.0 K (cold end of pulse tube, no load)
	Ultimate temperature	83.7 K (cold end of regenerator, no load)
	Mass flow at PWG	1.48 g/s
	Mass flow into regen	1.10 g/s
	Mass flow into PT	0.51 g/s

Run 2:	Frequency	19 Hz
	Average Pressure	1.68 MPa
	Pressure Ratio	not measured
	Pressure Ratio	1.29 (at hot end of pulse tube)
	Pressure Swing	7-10 KPa (hot end of pulse tube, operating)
	Inlet Temperature	305 K (at top plate)
	Ultimate temperature	84.4 K (cold end of pulse tube, no load)
	Ultimate temperature	87.0 K (cold end of regenerator, no load)
	Mass flow at PWG	1.80/s
	Mass flow into regen	1.35/s
	Mass flow into PT	0.62/s

The measured performance of the current baseline system for these two runs is shown in figures 3.3-1 and 3.3-2. The measured performance is lower than the predicted performance by a factor of about 2.2 which is believed to be related to the finite dead volume of the regenerator. The curves show a cooling power that rises linearly with increased operating temperature, and is:

12.9 deg/W for $P_{average}$ = 1.19 MPa

and

9.16 deg/W for $P_{average}$ = 1.68 MPa

The cooling power of the pulse tube is predicted to be proportional to mass flow, and the ratio of cooling power in Watts/deg is 1.41 and is within 20% of the ratios of the computed mass flows.

Taking the theoretical expression in eqn 3.2-1 and using the factor of 2.2 as a simple multiplicative factor, it is possible to predict the performance of the "best effort" system with PT-G installed. This prediction is shown in figure 3.3-3. This figure shows a computed cooling power of 0.2W at 80K. As of the end of the contract period, this measurement had not been made.

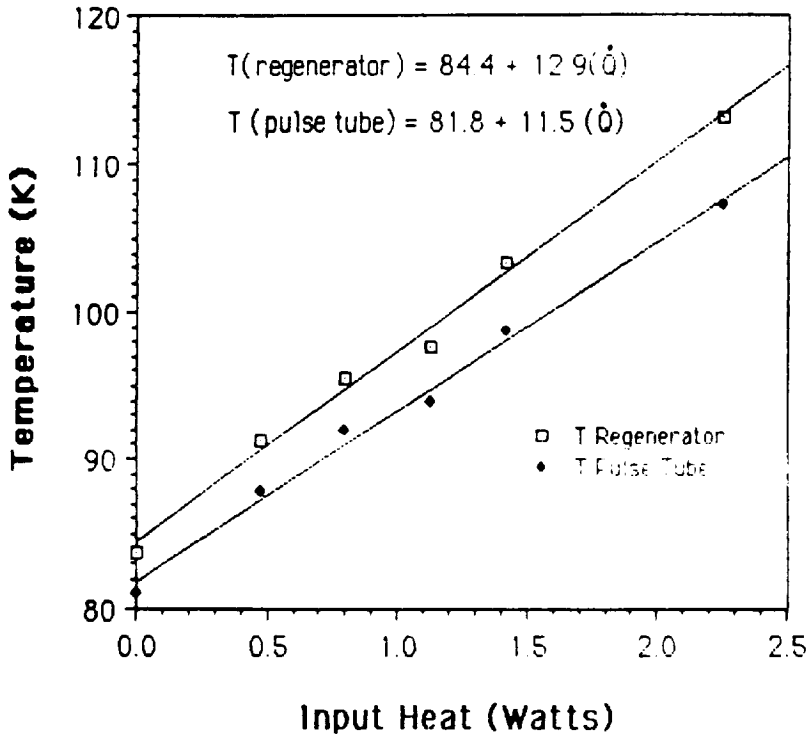

Figure 3.3-1 Measured cooling power as a function of temperature for an average pressure of 1.2 MPa.

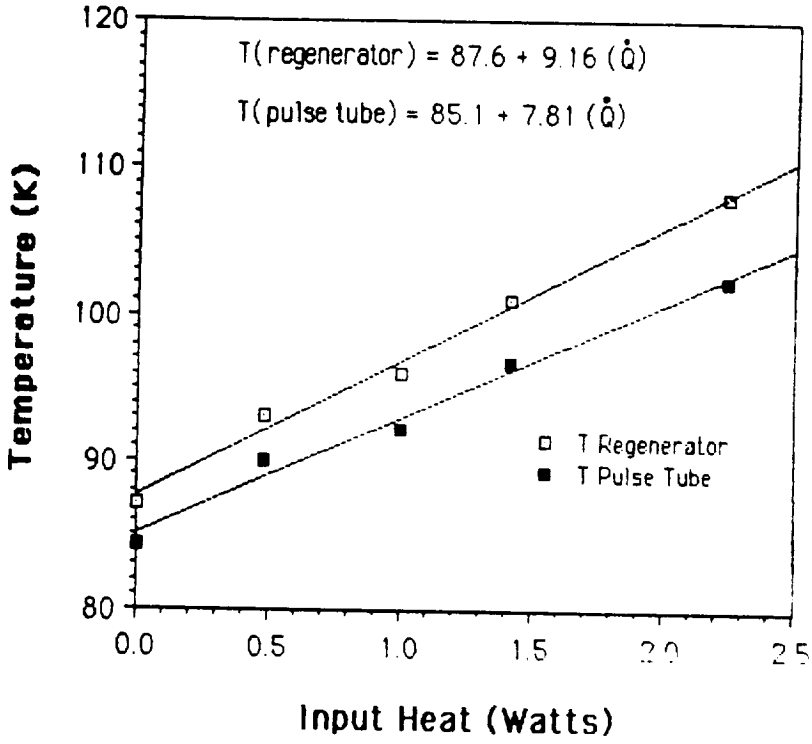

Figure 3.3-2 Measured cooling power as a function of temperature for an average pressure of 1.7 MPa.

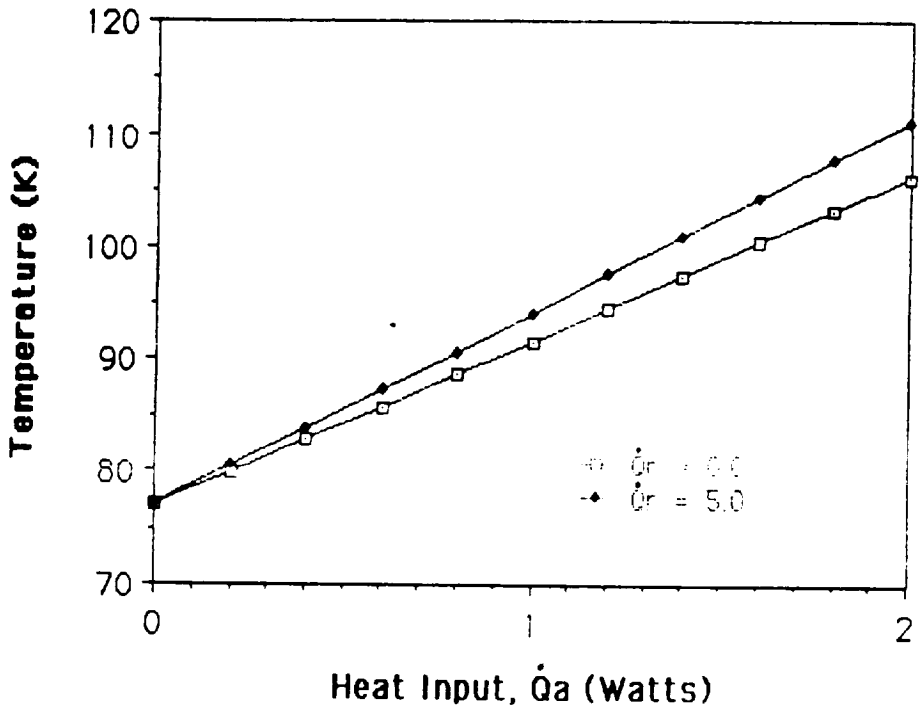

Figure 3.3-3 Predicted cooling power as a function of temperature for the current prototype using PT-G.

4.0 RESULTS AND CONCLUSIONS

This program has produced the following results:

a. A partially optimized pulse tube refrigerator has been developed that demonstrates an ultimate temperature of 77K, has a projected cooling power of 0.18 Watts at 80K, and a measured cooling power of 1 Watt at 97K, with an electrical efficiency of 250 Watts / Watt.

b. A simplified system model of the pulse tube refrigerator has been developed that provides a-priori estimates of pressure ratio and mass flow distribution within the pulse tube refrigerator, based on component physical characteristics. These estimates are accurate enough to drive the models of regenerator and pulse tube performance and operation.

c. A model of pulse tube operation has been developed based on generalized analysis. This model is adequate to support local optimization of existing systems, but is not yet sophisticated enough to support a-priori design.

d. A model of regenerator performance has been developed based on an analogy to counterflow heat exchangers. This model is again adequate for local optimization but not for a-priori design.

The analytical and experimental work in this program supports the following conclusions.

a. Practical pulse tube refrigerators with cooling powers in the range of 0 to 2 Watts are possible, and may be expected to exhibit specific inputs in the 100-250 Watts/Watt range at 90-100K and possibly as low as 70-80K.

b. Practical pulse tube refrigerators can be designed and built by starting with an initial cut and try design, and using the tools developed in this effort to support local modeling and optimization to develop the final design.

c. The a-priori design of pulse tube refrigerators remains extremely difficult because of the interactions of system components and the fact that none of the components operate under ideal conditions and adequate analytical solutions and approaches do not exist.

d. Some of the "magic" of the pulse tube remains unexplained and must be treated as rules-of-thumb, including:

   i. the gas from the warmest 1/3 of the pulse tube will be pushed into and out of the orifice volume on each stroke,
   ii. the pulse tube refrigerator will operate most efficiently when the volume of the pulse tube itself is approximately 1/3 of the effective volume of the driving pressure wave generator.

5.0 RECOMMENDATIONS

We recommend the following further development of the pulse tube refrigerator:

a. The existing partially optimized design should continue to be developed and optimized in a Phase III effort with private financing. The further optimization would logically include:

   i. reimplementing the regenerator in a perforated plate design, enhancing efficiency with the same dead volume, or reducing dead volume (and raising the pressure ratio) while maintaining constant efficiency,

   ii. reduce known system pressure drops, including those in the upper connecting line and the regenerator to improve system efficiency and reduce specific power input.

b. The existing design and analysis tools should be refined where possible, and attempts to develop a-priori design tools should not be abandoned, but should be focused on understanding the effects of pressure ratio on pulse tube performance, which is perhaps the least well understood facet of the analytical models.

6.0 REFERENCES

1. Gifford, W.E., and Longsworth, R.C., Pulse-Tube Refrigeration, ASME Paper No. 63-WA-290, (1963); Pulse Tube Refrigeration Progress, in: Advances in Cryogenic Engineering, 10B, (Plenum Press, New York, 1965), p. 69.

2. Incropera, F.P. and DeWitt, D.P., Fundamentals of Heat and Mass Transfer, 2nd ed., (John Wiley & Sons, 1985).

3. Jakob, M., Heat Transfer, Vol. II. (Wiley and Sons, New York, 1957), see Chapter 35, "Regenerators".

4. Jingtao Liang, Yuan Zhou, Wenxiv Zhu, Cryogenics, 30, p. 49.

5. Kays, W.M. and London, A.C., Compact Heat Exchangers, 3rd ed., (McGraw-Hill, 1984).

6. Levenspiel, O., Engineering Flow and Heat Exchange, (Plenum, New York, 1984).

7. Longsworth, R.C., "An Experimental Investigation of Pulse Tube Refrigeration Heat Pumping Rates", in: Advances in Cryogenic Engineering, 12, (Plenum Press, New York, 1967), p. 608.

8. Mikulin, E.L., Tarasov, A.A., and Shkrebyonock, M.P., "Low Temperature Expansion Pulse Tube", in: Advances in Cryogenic Engineering, 29, (Plenum Press, New York, 1984), p. 629.

9. Radebaugh, R., Advances in Cryogenic Engineering, 35 B, (Plenum Press), p. 1191.

10. Radebaugh, R. et al., "A Comparison of Three Types of Pulse Tube Refrigerators: New Methods for Reaching 60 K", in: Advances in Cryogenic Engineering, 31, (Plenum Press, New York, 1986), p. 779.

11. Rallis, C.J., Vurieli, I., and Berchowitz, D.M., "A New Mathematical Model for Stirling Cycle Machines, Proc. 12th I.E.C.E.C., Paper No. 779254, Washington, DC (1977).

12. Roth, A., Vacuum Technology, 2nd ed. Revised, (Northland-Holland, 1982).

13. Walker, G. Cryocoolers, (Plenum, New York, 1983).

14. Walker, G., Cryogenics, 19, p. 603, (1979).

15. Wheatley, J., Hoffer, G.W., Swift, and Migliori, A., "Understanding Some Simple Phenomena in Thermoacoustics with Applications in Acoustical Heat Engines", Am. J. Phys. 53, (1985) p. 147.

16. Zhu Shaowei, Wu Peiyi, and Chen Zhongqi, Cryogenics 30, 1990, p. 514.

NASA
National Aeronautics and Space Administration

Report Documentation Page

1. Report No.	2. Government Accession No.	3. Recipient's Catalog No.
Final	NAS7-1031	

4. Title and Subtitle

A Small Single Stage Orifice Pulse Tube Cryocooler Demonstration

5. Report Date

August 28, 1990

6. Performing Organization Code

ACE Inc.

7. Author(s)

Dr. John B. Hendricks, Principal Investigator
Dr. Myron E. Calkins, Project Scientist

8. Performing Organization Report No.

10. Work Unit No.

9. Performing Organization Name and Address

Alabama Cryogenic ENgineering, INc.
P.O. Box 2470
HUntsville, AL 35804

11. Contract or Grant No

NAS7-1031

13. Type of Report and Period Covered

3/2/88 - 8/2/90
Final Report

12. Sponsoring Agency Name and Address

National Aeronautics and Space Administration
Jet Propulsion Laboratory, 4800 Oak Grove Drive
Pasadena, CA

14. Sponsoring Agency Code

NASA/JPL

15. Supplementary Notes

16. Abstract

This final report summarizes and presents the analytical and experimental progress in the present effort. The principal objective of this effort was: "The demonstration of a 0.25 Watt, 80 Kelvin Orifice Pulse Tube Refrigerator."

The report includes: a) A description of the experimental apparatus; b) The design of a partially optimized pulse tube refrigerator. The refrigerator demonstrates an ultimate temperature of 77K has a projected cooling power of 0.18 Watts at 80K, and a measured cooling power of 1 Watt at 97K, with an electrical efficiency of 250 Watts / Watt, much better than previous pulse tube refrigerators; c) A model of the pulse tube refrigerator that provides estimates of pressure ratio and mass flow within the pulse tube refrigerator, based on component physical characteristics; d) A model of pulse tube operation based on generalized analysis and is adequate to support local optimization of existing designs; and e) A model of regenerator performance based on an analogy to counterflow heat exchangers.

17. Key Words (Suggested by Author(s))	18. Distribution Statement
Refrigerator cryocooler pulse tube regenerator heat exchanger	SBIR R&D-Restricted

19. Security Classif. (of this report)	20. Security Classif. (of this page)	21. No. of pages	22. Price
Proprietary / Unclassified	Proprietary / Unclassified	95	$474,707

NASA FORM 1626 OCT 86